© 2020. Published by The Company of Biologists Ltd | Journal of Cell Science (2020) 133, jcs244475. doi:10.1242/jcs.244475

CORRECTION

Correction: Alterations in the balance of tubulin glycylation and glutamylation in photoreceptors leads to retinal degeneration

Montserrat Bosch Grau, Christel Masson, Sudarshan Gadadhar, Cecilia Rocha, Olivia Tort, Patricia Marques Sousa, Sophie Vacher, Ivan Bieche and Carsten Janke

There was an error in *J. Cell Sci.* (2017) **130**, 938-949 (doi:10.1242/jcs.199091).

The authors incorrectly stated on p. 946 in the Materials and Methods that the *Ttll3*$^{-/-}$ strain was developed as described by Rocha et al. (2014). However, they actually used two strains, the one described in Rocha et al. (2014) and a new one that was generated by excising exon 6. The corrected text for the first paragraph of the Materials and Methods is as follows.

Animal experimentation

All wild-type control mice used in our experiments were C57BL/6 mice (Janvier-Europe). For experiments in mice lacking the TTLL3 gene, we used either the *Ttll3* mutant mice [European Mouse Mutant Archive (EMMA); mouse strain B6;B6-Ttll3<tm1a(EUCOMM)Wtsi>/Wtsi)] (Rocha et al., 2014), or *Ttll3*$^{-/-}$ mice. The latter were generated in two steps. First, we excised the *lacZ*-neomycin cassette *in vivo* by crossing B6;B6-Ttll3<tm1a(EUCOMM)Wtsi>/Wtsi) mice with a Flp-deleter line (C57BL/6N genetic background FLP under *ACTB* promoter), generating the *Ttll3*$^{flox/flox}$ strain. Next, we excised the exon 6 of *Ttll3*$^{flox/flox}$ mice by crossing them to mice expressing Cre recombinase under the control of a PGK promoter (Lallemand et al., 1998), thus generating the *Ttll3*$^{-/-}$ strain.

Reference

Lallemand, Y., Luria, V., Haffner-Krausz, R. and Lonai, P. (1998). Maternally expressed PGK-Cre transgene as a tool for early and uniform activation of the Cre site-specific recombinase. *Transgenic Res.* **7**, 105-112. doi:10.1023/a:1008868325009

The authors apologise to readers for this error, which does not impact the results or conclusions of the paper. Both the online full text and PDF versions of the article have been corrected.

© 2017. Published by The Company of Biologists Ltd | Journal of Cell Science (2017) 130, 938-949 doi:10.1242/jcs.199091

RESEARCH ARTICLE

Alterations in the balance of tubulin glycylation and glutamylation in photoreceptors leads to retinal degeneration

Montserrat Bosch Grau[1,2,*,], Christel Masson[3,**], Sudarshan Gadadhar[1,2], Cecilia Rocha[1,2,‡], Olivia Tort[1,2,§], Patricia Marques Sousa[1,2,¶], Sophie Vacher[4], Ivan Bieche[4,5] and Carsten Janke[1,2,‡‡]**

ABSTRACT

Tubulin is subject to a wide variety of posttranslational modifications, which, as part of the tubulin code, are involved in the regulation of microtubule functions. Glycylation has so far predominantly been found in motile cilia and flagella, and absence of this modification leads to ciliary disassembly. Here, we demonstrate that the correct functioning of connecting cilia of photoreceptors, which are non-motile sensory cilia, is also dependent on glycylation. In contrast to many other tissues, only one glycylase, TTLL3, is expressed in retina. *Ttll3*$^{-/-}$ mice lack glycylation in photoreceptors, which results in shortening of connecting cilia and slow retinal degeneration. Moreover, absence of glycylation results in increased levels of tubulin glutamylation in photoreceptors, and inversely, the hyperglutamylation observed in the Purkinje cell degeneration (*pcd*) mouse abolishes glycylation. This suggests that both posttranslational modifications compete for modification sites, and that unbalancing the glutamylation–glycylation equilibrium on axonemes of connecting cilia, regardless of the enzymatic mechanism, invariably leads to retinal degeneration.

KEY WORDS: Tubulin, Microtubule, Glutamylation, Glycylation, TTLL3, Retina, Photoreceptor, Connecting cilia

INTRODUCTION

Posttranslational modifications (PTMs) are essential modulators of protein functions. In the case of the cytoskeleton, microtubules (MTs) have been demonstrated to carry a panoply of different PTMs, some of which are referred to as 'tubulin PTMs' because they are particularly enriched on tubulin (reviewed in Janke, 2014). The best-characterized PTMs of tubulin are acetylation (of lysine 40 of α-tubulin; L'Hernault and Rosenbaum, 1985; Piperno et al., 1987), enzymatic detyrosination and re-tyrosination of α-tubulin (Arce et al., 1975; Hallak et al., 1977), and the posttranslational addition of glutamate and glycine chains to both, α- and β-tubulin, referred to as polyglutamylation (Eddé et al., 1990) and polyglycylation (Redeker et al., 1994). Most of these PTMs accumulate on long-lived, functionally specialized MTs (Cambray-Deakin and Burgoyne, 1987; Schulze et al., 1987), and are consequently enriched on the axonemes of cilia and flagella (Mary et al., 1996, 1997), on centrioles of the centrosome and the basal bodies (Bobinnec et al., 1998) and on neuronal MTs (Audebert et al., 1993, 1994). Despite their general abundance on stable MT assemblies, each PTM is expected to fulfil specific functions in the regulation of the MT cytoskeleton. The functional characterization of tubulin PTMs is an emerging field that has been strongly advanced by the discovery of many of the enzymes involved in tubulin acetylation (Akella et al., 2010; Shida et al., 2010), tyrosination (Ersfeld et al., 1993), polyglutamylation (Ikegami et al., 2006; Janke et al., 2005; Kimura et al., 2010; Rogowski et al., 2010; Tort et al., 2014; van Dijk et al., 2007) and polyglycylation (Ikegami and Setou, 2009; Rogowski et al., 2009; Wloga et al., 2009).

In the current study, we investigate the functions of a still barely understood PTM of MTs, glycylation, in the mouse retina, with a specific focus on the photoreceptors. Glycylation is, similar to glutamylation, generated by enzymes of the tubulin tyrosine ligase-like (TTLL) family (Janke et al., 2005; Rogowski et al., 2009; van Dijk et al., 2007; Wloga et al., 2009). So far no reverse enzyme (deglycylase) has been found for this PTM, while deglutamylases have been identified as members of a family of cytosolic carboxy peptidases (CCP; Kimura et al., 2010; Rogowski et al., 2010; Tort et al., 2014).

The discovery of these enzymes has already allowed a number of functional studies, which have provided first insights into the functions of glutamylation and glycylation. For instance, we have shown that the balance between glutamylation and deglutamylation is essential for the survival of neurons (Rogowski et al., 2010). The mutation of CCP1 (also known as AGTPBP1), a key deglutamylase, leads to compromised deglutamylation in a mouse model for Purkinje cell degeneration (*pcd*; Mullen et al., 1976), which results in hyperglutamylation and neurodegeneration of the affected neurons (Rogowski et al., 2010). MT glutamylation and glycylation are particularly important in cilia and flagella. Both PTMs are strongly enriched on the MT core structure of these organelles, the axoneme (Bré et al., 1996). Observations in a variety of model organisms suggest that in motile cilia or flagella, glutamylation controls the beating behaviour of these organelles (Bosch Grau et al., 2013; Ikegami et al., 2010; Janke et al., 2005; Kubo et al., 2010; Pathak et al., 2011; Suryavanshi et al., 2010). The above-mentioned *pcd* mouse for instance, which accumulates pathological levels of polyglutamylation, is male-sterile due to dysfunctions of the sperm flagellum (Handel and Dawson, 1981).

Glycylation, on the other hand, stabilizes axonemes. RNAi-mediated depletion of a key glycylase enzyme in *Drosophila*

[1]Institut Curie, PSL Research University, CNRS UMR3348, Orsay F-91405, France. [2]Université Paris Sud, Université Paris-Saclay, CNRS UMR3348, Orsay F-91405, France. [3]CERTO Centre d'Etudes et de Recherches Thérapeutiques en Ophtalmologie, Université Paris Sud, Université Paris-Saclay, CNRS UMR9197, Orsay F-91405, France. [4]Institut Curie, PSL Research University, Department of Genetics, Paris F-75005, France. [5]Université Paris Descartes, Sorbonne Paris Cité, Paris F-75005, France.
*Present address: Institut Pasteur, Laboratory of Genetics and Physiology of Hearing, INSERM UMRS1120, Paris F-75724, France. ‡Present address: Department of Biology, McGill University, Montréal, Québec, Canada H3A 1B1. §Present address: Institut d'Investigacions Biomèdiques August Pi i Sunyer (IDIBAPS), Hospital Clínic de Barcelona, Barcelona E-08036, Spain. ¶Present address: Harvard Medical School, Children's Hospital Boston, Boston, MA 02115, USA.
**These authors contributed equally to this work

‡‡Author for correspondence (Carsten.Janke@curie.fr)

P.M.S., 0000-0002-6045-4077; C.J., 0000-0001-7053-2000

Received 2 November 2016; Accepted 10 January 2017

Journal of Cell Science (2017) 130, 938-949 doi:10.1242/jcs.199091

melanogaster testes leads to a progressive disassembly of the sperm axonemes (Rogowski et al., 2009), and knockout or RNAi-mediated depletion of the two mammalian glycylases TTLL3 and TTLL8 in mouse ependymal cells (Bosch Grau et al., 2013) leads to ciliary disassembly. Even primary cilia, which appear to be much less glycylated than motile cilia, require glycylation to function correctly (Rocha et al., 2014). It thus seems that there are selective functions for both PTMs in cilia; glycylation is regulating the stability of the MT assembly, while glutamylation might regulate the motor proteins that interact with the axoneme, thus controlling the ciliary beating and/or the intraflagellar transport (IFT; Broekhuis et al., 2013).

A functionally highly specialized type of cilium is found in the photoreceptor cells of the eye retina. In mouse, cone photoreceptors develop between embryonic day (E)11.5 and E18, whereas rod photoreceptor cells, which constitute 97% of all photoreceptor cells in the adult retina, differentiate only after birth (LaVail, 1973; Morrow et al., 1998). In mice, the rod outer segment elongates at a rapid and almost linear rate from postnatal day (P)11 to P17, reaching its final length by P19–P25 (LaVail, 1973). A unique bridge – the connecting cilium – connects outer and inner segments of photoreceptor cells.

Here, we investigate the link between photoreceptor development and the dynamics of polyglycylation and polyglutamylation in the photoreceptor connecting cilia. Using a knockout mouse model for the glycylase TTLL3, we demonstrate that changes in the levels of glycylation lead to hyperglutamylation, followed by progressive degeneration of the photoreceptors. This situation is comparable to that of the *pcd* mouse model, which has earlier been shown to develop retinal degeneration (Blanks et al., 1982; Blanks and Spee, 1992; LaVail et al., 1982). Our data demonstrate that both glycylation and glutamylation are enriched at the photoreceptor connecting cilium, and that they influence each other. Their strict control appears to be essential for the maintenance and survival of photoreceptors, and deregulation of either of these PTMs leads to retinal degeneration.

RESULTS

A differential timing of tubulin glycylation and glutamylation during photoreceptor development

To determine the dynamics of tubulin glycylation and glutamylation during postnatal development and maturation, we characterized mouse retina by immunohistochemistry with an antibody specific for glycylation (TAP952; Bré et al., 1996), or with the glutamylation marker GT335 (Wolff et al., 1992). Mouse retinas dissected and fixed at P1, P6, P10, P15 and P60 were immunostained either with TAP952 or with GT335, and co-stained with a marker for basal bodies and connecting cilia (pan-centrin 20H5; Giessl et al., 2004; Sanders and Salisbury, 1994; Trojan et al., 2008) and for tubulin (C105, specific to β-tubulin; Arevalo et al., 1990).

Starting from P1 (before the development of the outer segment) and throughout photoreceptor development, the glutamylation-specific antibody GT335 selectively labelled structures that were also labelled with the centrin marker. While in P1 these structures are most likely the centrioles, they are considered as the connecting cilia from P6 onwards (Fig. 1A). Glutamylation was also detected at the inner segments (Fig. 1A) in all stages of development, but was, however, much weaker than the strong labelling of the connecting cilia.

Glycylation (TAP952 labelling), on the other hand, was absent from immature photoreceptors at P1 (Fig. 1B,C), and was first detected at P6, before the outgrowth of the outer segments, in some, but not all, centrin-positive structures. In later stages, especially after P10, which marks the starting point for the rapid elongation of the outer segment, all connecting cilia, as well as the proximal part of the outer segments were labelled with TAP952 (Fig. 1B,C). In contrast to glutamylation, glycylation was absent from other cellular MT structures in the photoreceptor. This pattern of TAP952 labelling persisted throughout all stages of development.

Thus, the glutamylation of photoreceptor connecting cilia is generated concomitantly with their assembly, and glutamylation also might occur in basal bodies (Fig. 1D), whereas glycylation is gradually generated with the assembly of the connecting cilia, and is fully established after the elongation of the outer segments.

TTLL3 is the sole initiating glycylase enzyme expressed in mouse retina

Glutamylation and glycylation are both catalysed by enzymes from the TTLL family. Nine glutamylases have been identified in mammals (van Dijk et al., 2007), whereas only three glycylases exist. Two of them, TTLL3 and TTLL8, catalyse the initial addition of glycine residues to tubulin, whereas TTLL10 uniquely elongates preformed glycine side chains on tubulin (Rogowski et al., 2009). Thus, TTLL3 and/or TTLL8 are essential to initiate tubulin glycylation, and absence of both enzymes is expected to lead to complete loss of tubulin glycylation. To determine which of these two enzymes is expressed in retina, we performed reverse transcription followed by quantitative real-time PCR (qRT-PCR) at a range of developmental stages (P0 to 1-year-old mice). Strikingly, expression of only one initiating glycylase, TTLL3 was detectable in retina at all developmental stages analysed (Fig. S1). Increased TTLL3 expression during retina development is coherent with the observed increase of glycylation during retina maturation (Fig. 1B). Thus, glycylation observed in photoreceptor cells is most likely generated by TTLL3 alone. The expression of TTLL3 in the retina was further confirmed by *in situ* hybridization, where strong hybridization signals were obtained in the photoreceptor cells (Fig. S2).

Absence of tubulin glycylation leads to hyperglutamylation in photoreceptor cells

As glycylation in the mouse retina is catalysed exclusively by TTLL3, we investigated the role of this PTM in our TTLL3-knockout (*Ttll3*$^{-/-}$) mouse (Bosch Grau et al., 2013; Rocha et al., 2014). We first confirmed the absence of TTLL3 expression in retina of *Ttll3*$^{-/-}$ mice at different developmental stages, and demonstrated that TTLL8 expression remained virtually undetectable, similar to in the wild-type situation (Fig. S1). This indicates that TTLL8 is not upregulated to compensate for the lack of TTLL3. The absence of both glycylases should lead to a total absence of glycylation in the photoreceptors, which we confirmed by immunohistochemistry with TAP952. In *Ttll3*$^{-/-}$ retinas, no TAP952 staining was detected in photoreceptors of 5-week- and 4-month-old mice (Fig. S3A), whereas the connecting cilia were strongly labelled in comparable control retinas (Fig. 1B).

Previous work had indicated that tubulin glutamylation and glycylation affect each other, as both modifications use similar modification sites on the tubulin C-terminal tails (Rogowski et al., 2009; Wloga et al., 2009). To investigate whether the absence of glycylation in the *Ttll3*$^{-/-}$ retina leads to altered levels of tubulin glutamylation in photoreceptor cells, we analysed retina sections from P15, 5-week-old, 4- and 12-month-old wild-type and *Ttll3*$^{-/-}$ mice with the antibodies GT335 for tubulin glutamylation (Wolff et al., 1992), or for polyglutamylation (denoted polyE) (Magiera

Journal of Cell Science (2017) 130, 938-949 doi:10.1242/jcs.199091

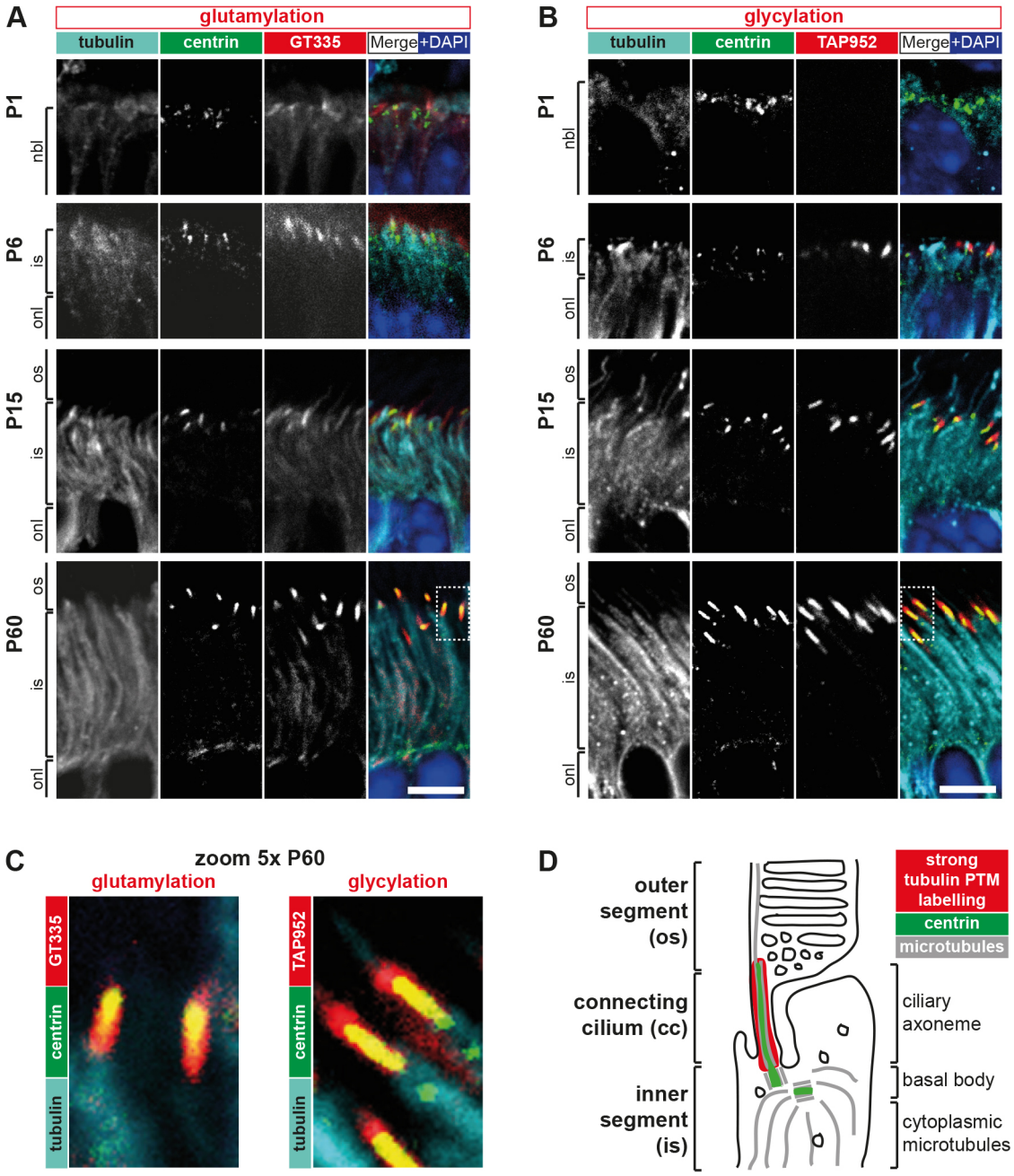

Fig. 1. Glutamylation and glycylation in developing photoreceptors. (A) Co-immunostaining of wild-type retina sections at different postnatal ages with pan-centrin antibody (20H5; green), β-tubulin (C105; cyan) and anti-glutamylation GT335 (red). Nuclei are visualized with DAPI (blue). Glutamylated tubulin is present in the connecting cilium (defined by centrin; 20H5 staining) from the onset of ciliogenesis at P1. (B) Immunostaining as in A with the red channel showing glycylation (TAP952). Glycylation is absent from immature photoreceptors (P1), begins to appear in some of the nascent connecting cilia at P6, and is present in all connecting cilia from P15 onwards. nbl, neuroblastic layer; is, inner segment; os, outer segment; onl, outer nuclear layer. (C) Zoom (5×) from merged images from P60 from A and B. Note that both glutamylation and glycylation signals colocalize with the centrin staining. (D) Schematic representation of the distributions of PTMs in mature photoreceptor cell. Scale bars: 5 µm.

and Janke, 2013; Rogowski et al., 2010; Shang et al., 2002; Wloga et al., 2008). An antibody for β-tubulin (C105) was used to co-stain the MT network, and a pan-centrin antibody (20H5) to specifically visualize connecting cilia and basal bodies (Fig. 2).

We then measured the intensity of GT335 and polyE staining using ImageJ (Fig. 3), and quantified labelling intensities of all MTs of the photoreceptor cells (Fig. 2), including MTs in the inner segment, the connecting cilium and the basal body (Fig. 1D). In 5-week-old retinas, the GT335 labelling was increased threefold in *Ttll3*$^{-/-}$ mice as compared to controls (Figs 2A and 3A), while the polyE signal was not significantly increased (Figs 2B and 3B). After 4 months, however, the polyE signal of the connecting cilia was increased threefold in *Ttll3*$^{-/-}$ retinas (Figs 2B and 3B). This indicates that the absence of glycylation indeed allows hyperglutamylation of the MTs in photoreceptor cells. The generation of long glutamate chains takes place progressively, and longer glutamate chains accumulate only after several months, whereas shorter glutamate side chains have already accumulated during the early photoreceptor development in *Ttll3*$^{-/-}$ mice.

Journal of Cell Science (2017) 130, 938-949 doi:10.1242/jcs.199091

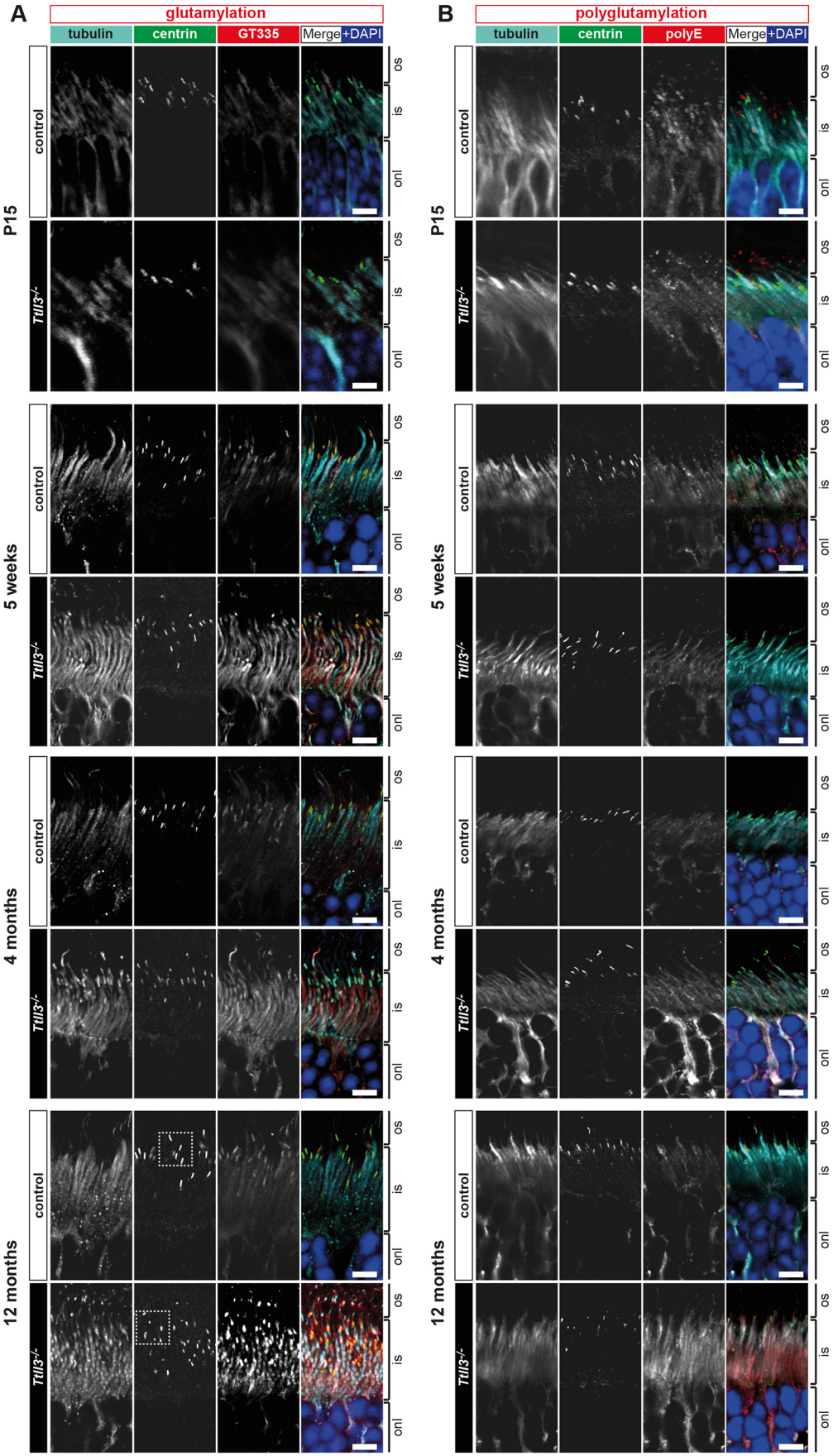

Fig. 2. Absence of glycylation leads to increase in glutamylation in photoreceptors of *Ttll3*$^{-/-}$ mice. (A) Co-immunostaining of retina sections from control and *Ttll3*$^{-/-}$ mice at different postnatal ages with pan-centrin antibody (20H5; green), β-tubulin (C105; cyan) and anti-glutamylation GT335 (red). Nuclei are visualized with DAPI (blue). The GT335 labelling becomes stronger in the *Ttll3*$^{-/-}$ mouse as compared to control starting from 5 weeks. A zoom of the boxed regions (12 months) is shown in Fig. 3C. (B) Immunostaining as in A; the red channel representing polyglutamylation (polyE), and tubulin labelled with DM1A. The polyE labelling becomes stronger in *Ttll3*$^{-/-}$ mouse as compared to control only after 4 months. is, inner segment; os, outer segment; onl, outer nuclear layer. Scale bars: 5 µm.

Journal of Cell Science (2017) 130, 938-949 doi:10.1242/jcs.199091

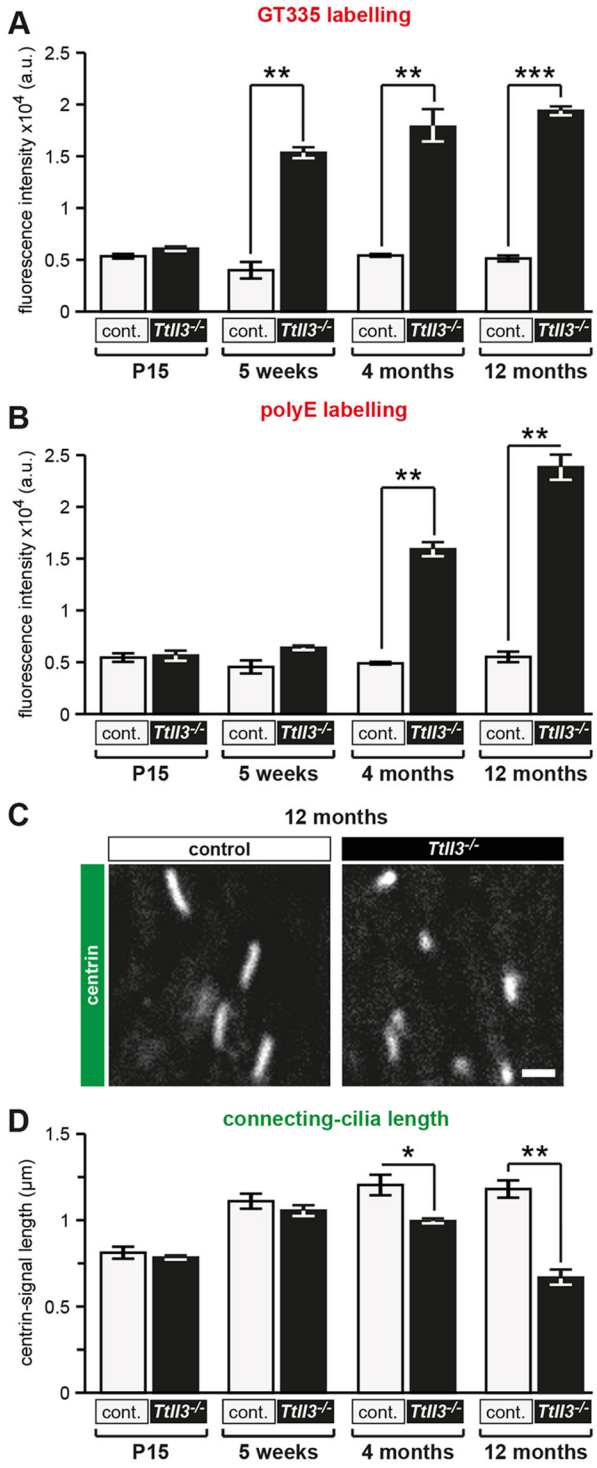

Fig. 3. Quantification of glutamylation and connecting-cilia length in *Ttll3*$^{-/-}$ retinas. Fluorescence intensities of (A) GT335 and (B) polyE labelling of the photoreceptor cell layer (as shown in Fig. 2) were quantified from maximum projection stacks using ImageJ. Square ROIs including inner and outer segments of photoreceptors were defined, and the mean values of the ROI in the GT335 channel were determined for each image. (C) Zoomed view of boxed region in Fig. 2A. (D) The length of the connecting cilium was quantified on image stacks taken from whole-mount retina preparations stained with anti-centrin (20H5; as shown in C), using the ObjectJ plugin from ImageJ, on P15, 5-week-old, and 4- and 12-month-old animals. All panels show mean±s.e.m. obtained from three independent animals per time point analysed. *P<0.05, **P<0.01, ***P<0.001 (multiple comparisons were performed by Student's t-test).

The observed increase of glutamylation in *Ttll3*$^{-/-}$ retinas is not due to changes in the expression of glutamylating and/or deglutamylating enzymes, as we quantified expression levels of all known enzymes at different developmental stages, and none of them showed significantly altered expression levels in *Ttll3*$^{-/-}$ versus wild-type retinas (Fig. S1). We further verified the glycylation and glutamylation status of the retinitis pigmentosa GTPase regulator (RPGR), which is modified by the glutamylase TTLL5, and had been shown to be at the origin of retinal degeneration in *Ttll5*$^{-/-}$ mice (Sun et al., 2016). In retina extracts from control and *Ttll3*$^{-/-}$ mice, an ∼250 kDa strongly GT335-positive protein was detected; however, no protein of this size was detected with TAP952 (Fig. S3B). This indicates that this protein, most likely RPGR, is not glycylated, and its glutamylation levels are not altered in the absence of TTLL3. Thus, the lack of tubulin glycylation in *Ttll3*$^{-/-}$ mice mostly affects the tubulin in the photoreceptor cells, and causes progressive hyperglutamylation due to liberation of modification sites.

Glycylation controls the length and functionality of photoreceptor connecting cilia

To determine the role of tubulin glycylation on photoreceptor axonemes, we measured the length of the connecting cilia at distinct postnatal stages. We used the immunohistochemical analysis in which we had labelled the connecting cilium with the antibody 20H5 in retina sections at P15, 5-week, 4- and 12-month-old mice (Fig. 2) for these analyses. The length of the axoneme of connecting cilia was determined by measuring the centrin (20H5) labelling, which in photoreceptors shows a specific labelling of the connecting cilia (Giessl et al., 2004; Trojan et al., 2008). Control staining to ensure the correct orientation of the retina sections during length measurements were performed (Fig. S4A).

While in retinas from young mice (P15, 5-week-old) no obvious difference was determined, the connecting cilia were 17.2% shorter in 4-month-old, and 43.2% in 12-month-old *Ttll3*$^{-/-}$ mice as compared to the wild-type controls (Fig. 3C,D). Thus, the shortening of connecting cilia in photoreceptors lacking glycylation is a progressive process that occurs concomitantly with the increase of tubulin polyglutamylation in these cells (polyE labelling in Fig. 2B). Strikingly, despite the shortening of the connecting cilia, the size of the outer segments remained apparently unaltered up to 14 months (Fig. S4A).

Retina lacking glycylation shows signs of progressive photoreceptor degeneration

As shortening of connecting cilia could be a sign of retinal degeneration (Karlstetter et al., 2014), we analysed retinas of *Ttll3*$^{-/-}$ mice for signs of degeneration. First, we determined the distribution of rhodopsin in retina sections of 12-month-old mice. In control retinas, rhodopsin was exclusively localized within the photoreceptor outer segments. In contrast, ectopic rhodopsin labelling was present at the nuclear layer of the photoreceptor cells of *Ttll3*$^{-/-}$ mice (Fig. 4A), which is indicative of degeneration of the affected photoreceptors (Alfinito and Townes-Anderson, 2002).

Another marker for photoreceptor degeneration is the induction of retinal reactive gliosis in Müller cells and astrocytes as a result of increased stress in the retina (Honjo et al., 2000; Iandiev et al., 2006), which can be visualized by staining for the glial fibrillary acidic protein (GFAP). Indeed, we found a strong increase in GFAP labelling in retinas of 12-month-old *Ttll3*$^{-/-}$ mice as compared to controls (Fig. 4B). Finally, we performed terminal deoxynucleotidyl transferase dUTP nick-end-labelling (TUNEL) analyses on 4- and

Journal of Cell Science (2017) 130, 938-949 doi:10.1242/jcs.199091

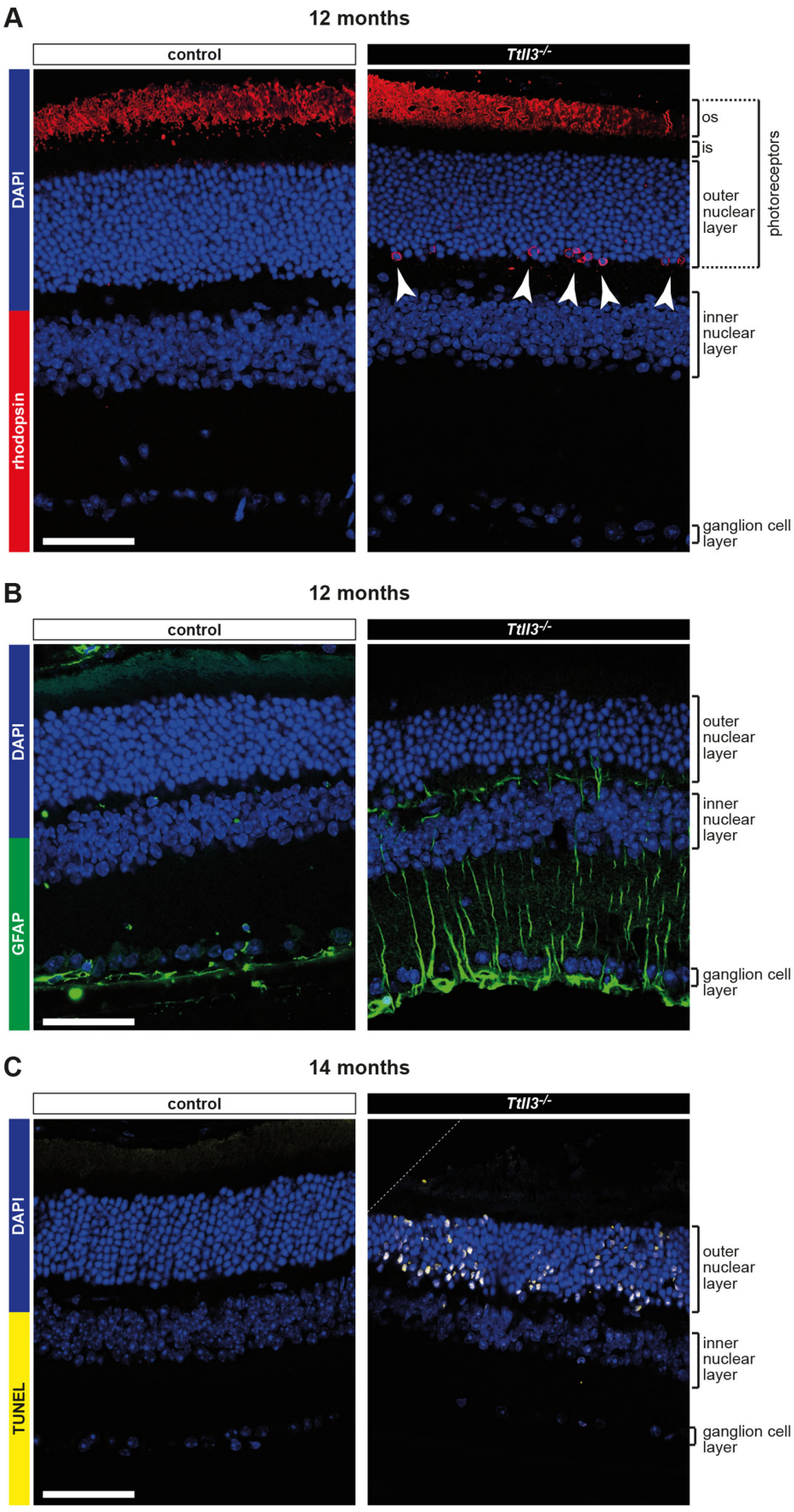

Fig. 4. Rhodopsin mislocalization, glia activation and apoptosis in *Ttll3*$^{-/-}$ retinas. Immunofluorescence analyses were performed with different markers of retinal degeneration on sections of the medial area of the retinas of 12- or 14-month-old control and *Ttll3*$^{-/-}$ mice. (A) Rhodopsin was labelled with anti-rhodopsin antibody (red). Note that rhodopsin staining is only found in the outer nuclear layer in *Ttll3*$^{-/-}$ retinas (arrowheads). (B) GFAP staining (green) was used to visualize activation of Müller glia cells. Note the strong GFAP staining in *Ttll3*$^{-/-}$ retinas. (C) TUNEL staining (yellow) to detect apoptosis in the photoreceptor cell layer. Note the strongly increased labelling in *Ttll3*$^{-/-}$ retinas. Nuclei in all panels are stained with DAPI (blue). is, inner segment; os, outer segment. Scale bars: 50 µm.

Journal of Cell Science (2017) 130, 938-949 doi:10.1242/jcs.199091

14-month-old retina sections from *Ttll3*$^{-/-}$ and control mice to detect apoptosis. While no differences were seen at 4 months (data not shown), many TUNEL-positive cells were detected in 14-month-old *Ttll3*$^{-/-}$ retinas specifically at the photoreceptor cell layer (Fig. 4C).

Thus, retinas of *Ttll3*$^{-/-}$ mice are positive for three independent markers of photoreceptor degeneration, which strongly suggests that the loss of tubulin glycylation and the resulting defects in connecting cilia lead to retinal degeneration in older mice. Indeed, the outer nuclear layer of the retina becomes visibly thinner in 16-month-old *Ttll3*$^{-/-}$ mice (Fig. S4B).

Hyperglutamylation in *pcd* mice reproduces the *Ttll3*$^{-/-}$ phenotype

The Purkinje cell degeneration (*pcd*3J) mouse (Mullen et al., 1976) carries a mutation in the *AGTPBP1* gene (Fernandez-Gonzalez et al., 2002) that encodes CCP1, a deglutamylase enzyme (Rogowski et al., 2010). The *pcd*3J mutation leads to a loss of CCP1 expression, resulting in hyperglutamylation in some brain regions, notably in the cerebellum, where massive neurodegeneration takes place. Strikingly, *pcd* mice also show progressive degeneration of photoreceptors, which starts at P15, when the first pyknotic nuclei can be observed in photoreceptors. Between 3 and 5 weeks of age, 50% of the photoreceptors are lost, and degeneration is complete after 1 year (Blanks et al., 1982; Chang et al., 2002; LaVail et al., 1982; Mullen and LaVail, 1975).

To compare the status of tubulin PTMs in *pcd* and *Ttll3*$^{-/-}$ mice, we analysed tubulin glycylation and glutamylation in the retina of the *pcd* mice. At P19, before the onset of photoreceptor degeneration, tubulin glutamylation in the photoreceptors of *pcd* mice was similar to that in control, and connecting cilia were glycylated as in control (Fig. 5A). In contrast, at P30, when degeneration is observed in *pcd* mice retinas (Chang et al., 2002), polyglutamylation levels were strongly increased, while the glycylation had disappeared from the connecting cilia (Fig. 5B). In addition, connecting cilia were 36.4% shorter in P30 *pcd* mice than in wild-type controls (Fig. 5C,D).

These results show that a balance between polyglutamylation and glycylation at the axonemes of the connecting cilia is essential for the maintenance of this particular part of photoreceptor cilia, and perturbing this balance towards hyperglutamylation invariably leads to photoreceptor degeneration. In *pcd* mice, hyperglutamylation accumulates much faster than in *Ttll3*$^{-/-}$ mice and consequently the process of photoreceptor degeneration, as measured by the shortening of the connecting cilia, is accelerated in the *pcd* mice. This suggests that the degree of deregulation of tubulin PTMs in photoreceptor connecting cilia correlates with the severity of retinal degeneration. Alternatively, other MTs in the photoreceptor cells, as well as other proteins important for photoreceptor function (Sun et al., 2016) might be hyperglutamylated in the *pcd* mice, thus accelerating the degenerative process.

DISCUSSION

Despite their great functional diversity, all cilia and flagella of eukaryotes are built of a highly conserved structural backbone, the axoneme. Axonemes, which are assembled from nine MT doublets, are essential for the mechanic and structural integrity of cilia, and are the railroads for IFT (Hao and Scholey, 2009). Axonemal tubulin is particularly rich in tubulin PTMs (reviewed in Konno et al., 2012), suggesting an important role for these modifications in ciliary assembly, maintenance and function. Glycylation and glutamylation are highly enriched in cilia and flagella of most eukaryotic organisms studied so far. Glycylation, which has exclusively been found on axonemal MTs, was shown to be important for ciliary integrity, as depletion of this PTM in different model organisms led to disassembly of motile cilia or flagella (Bosch Grau et al., 2013; Rogowski et al., 2009; Wloga et al., 2009). Polyglutamylation, on the other hand, regulates ciliary beating by controlling axonemal dynein motors (Bosch Grau et al., 2013; Ikegami et al., 2010; Kubo et al., 2010; Suryavanshi et al., 2010). Glutamylation can also be involved in length-control of cilia, as *Chlamydomonas* mutants lacking *TTLL9* have a reduced rate of axoneme shortening (Kubo et al., 2015), while excessive levels of TTLL6 lead to ciliary shortening in *Tetrahymena* (Wloga et al., 2010). Furthermore, glutamylation is also implicated in the control of IFT. In *C. elegans*, strains lacking the deglutamylase CCPP-1 show aberrant velocity and localization of two ciliary kinesins OSM-3 and KLP-6 (O'Hagan et al., 2011), and lack of DYF-1 also leads to a loss of OSM-3 motility (Ou et al., 2005). DYF-1 is the homolog of the zebrafish protein fleer, an IFT core complex B protein with a strong impact on glutamylation and glycylation in cilia (Pathak et al., 2007). Strikingly, the severity of the ciliary phenotypes depended on the co-depletion of glutamylation and glycylation in the fleer mutant, as the knockdown of either the ciliary glutamylase *TTLL6* or the glycylase *TTLL3* alone resulted in less-defective cilia. This indicates that both PTMs can cooperate in maintaining ciliary structure and function (Pathak et al., 2011).

Vertebrate photoreceptors contain one of the most specialized forms of cilia. These modified sensory cilia consist of a connecting cilium between the inner and the outer segment of the photoreceptor cell (Fig. 1D), which represents an extended version of the transition zone found in all primary cilia (Anand and Khanna, 2012; Reiter et al., 2012). While primary cilia are slender organelles that protrude from the cell surface, connecting cilia provide a unique link between the cell body of the photoreceptor, where the entire protein synthesis machinery is localized, with the light-sensing outer segment, which is devoid of protein synthesis (Wensel et al., 2016). Considering the sheer size of the outer segment, it appears that among all different variants of cilia, the connecting cilia of photoreceptors might be the cilia with the single most solicited IFT machinery (Wright et al., 2010). On the other hand, photoreceptors are tightly packed into the tissue of the retina, thus the connecting cilia might, in contrast to other cilia, experience little external mechanical stress.

Similar to in the motile ependymal cilia (Bosch Grau et al., 2013), glutamylation in connecting cilia is concomitantly generated with the cilia, whereas glycylation appears with a short delay. This was strongly indicative of a functional conservation of glycylation between motile and photoreceptor connecting cilia. We had previously shown that the two initiating glycylases, TTLL3 and TTLL8, are redundant in generating glycylation (Bosch Grau et al., 2013; Rogowski et al., 2009). As only TTLL3 was expressed in photoreceptors – a rare physiological situation previously only observed in colon (Rocha et al., 2014) – glycylation was entirely absent from connecting cilia of *Ttll3*$^{-/-}$ mice. However, in contrast to the motile cilia (Bosch Grau et al., 2013), connecting cilia did not disassemble in the absence of glycylation, most likely due to the absence of mechanical stress in an intact retina. Nevertheless, in older mice connecting cilia become shorter, which is indicative of progressive, but very slow disassembly of the axonemes. This strengthens the hypothesis that glycylation is involved in mechanically stabilizing axonemes, and shows that this function is not restricted to motile cilia.

Polyglutamylation increases concomitantly with the absence of glycylation, which makes it hard to determine which of the two PTMs is primarily responsible for the observed phenotypes. A

Journal of Cell Science (2017) 130, 938-949 doi:10.1242/jcs.199091

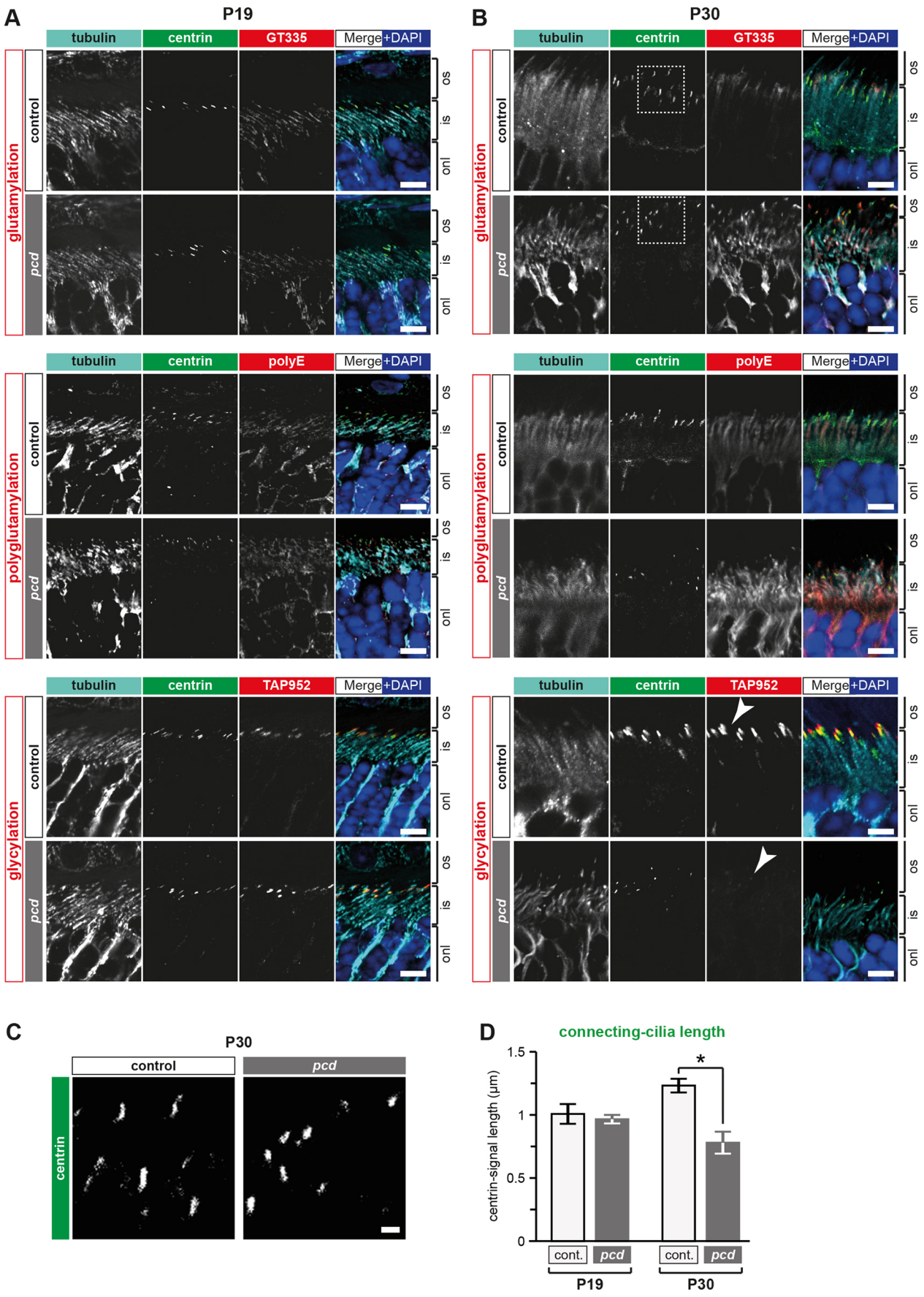

Fig. 5. See next page for legend.

Journal of Cell Science

Journal of Cell Science (2017) 130, 938-949 doi:10.1242/jcs.199091

Fig. 5. Hyperglutamylation in *pcd* mice reproduces the *Ttll3*$^{-/-}$ phenotype. Co-immunostaining of retina sections from control and *pcd* mice at postnatal ages P19 (A) and P30 (B) with pan-centrin antibody (20H5; green), combined with anti-PTM antibodies (red; glutamylation: GT335, polyglutamylation: polyE, glycylation: TAP952) and tubulin (C105, DM1A; cyan). Nuclei are visualized with DAPI (blue). While PTM levels are similar at P19, glutamylation and polyglutamylation are increased in *pcd* retinas at P30, whereas glycylation is strongly decreased (arrowheads). is, inner segment; os, outer segment; onl, outer nuclear layer. Scale bar: 5 µm. (C) Zoom of boxed regions in B. (D) The length of the connecting cilium was quantified on image stacks of whole-mount retina preparations stained with anti-centrin (20H5), using the ObjectJ plugin from ImageJ. Note that the length of the connecting cilia is reduced in retinas of P30 *pcd* mice. Mean±s.e.m. of three different animals are shown. **P*<0.05 (*t*-test).

competition of these two tubulin PTMs has been reported before (Rogowski et al., 2009; Wloga et al., 2009), and is most likely related to the use of identical modification sites on tubulin. In the *pcd* mouse, hyperglutamylation leads to a complete loss of glycylation; however, hyperglutamylation accumulates much faster than in the *Ttll3*$^{-/-}$ mice, and accordingly, the connecting cilia become shorter at earlier time points. This might explain why the degeneration of photoreceptors is more pronounced in the *pcd* mouse (LaVail et al., 1982) as compared to in the *Ttll3*$^{-/-}$ mouse. A possible conclusion is that the degree of hyperglutamylation correlates with the severity of degeneration, similar to what has been observed for the degeneration of different brain regions in *pcd* mice (Rogowski et al., 2010). Alternatively, the absence of the deglutamylase CCP1 could have a stronger functional impact because this enzyme reverses the glutamylation generated by several polyglutamylases, each of them having a distinct function in photoreceptor cells. For example, the glutamylase TTLL5, which has been found mutated in human retinopathies (Bedoni et al., 2016), specifically modifies the X-linked protein RPGR. The massive degeneration of photoreceptors in the *Ttll5*$^{-/-}$ mice was shown to result from the absence of glutamylation of RPGR rather than from aberrant tubulin glutamylation (Sun et al., 2016). In contrast, glutamylation of RPGR is normal in the *Ttll3*$^{-/-}$ mice; however, we cannot exclude that other, as yet unidentified, substrates of TTLL3 contribute to the observed phenotypes.

Our study shows that mutation of a single glycylase gene, *Ttll3*, is sufficient to induce slow retinal degeneration in mice, as revealed by shortened connecting cilia (Karlstetter et al., 2014), a massive activation of Müller glia, indicative of retinal stress (Honjo et al., 2000; Iandiev et al., 2006), and a remarkable increase of photoreceptor apoptosis. The degeneration could be related to a partial dysfunction of the IFT in the connecting cilia, which is considered a possible cause of retinal degeneration (Alfinito and Townes-Anderson, 2002; Boubakri et al., 2016; Bujakowska et al., 2015; Hollingsworth and Gross, 2012; Jiang et al., 2009). Indeed, a number of photoreceptors showed abnormalities in rhodopsin localization in retinas of old *Ttll3*$^{-/-}$ mice. The phenotype of the *Ttll3*$^{-/-}$ mouse is of particular interest for the research on human retina dysfunctions as (1) it represents an isolated phenotype (i.e. no other organ dysfunction has so far been found in *Ttll3*$^{-/-}$ mice), and (2) because it is a slow process, thus reproducing a number of human eye diseases that lead to progressive, slow degeneration of the retina (Veleri et al., 2015). The recent discovery of a *CCP5* (also known as *AGBL5*) as a candidate gene for retinitis pigmentosa in five patients (Kastner et al., 2015) further underpins the emerging role of tubulin-modifying enzymes as causative factors of retina disorders.

On the conceptual level, our work provides further evidence for the role of tubulin glycylation and glutamylation in the fine-tuning of MT functions. By comparing the *Ttll3*$^{-/-}$ and *pcd* (*Ccp1*$^{-/-}$) mouse models, we demonstrate that the degree of deregulation of these PTMs correlates with the severity of the resulting retinal degeneration. Our work thus demonstrates how alterations in different tubulin-modifying enzymes can generate a range of phenotypic alterations, from a slowly progressing degeneration of the retina in *Ttll3*$^{-/-}$ mice to a massive retinal degeneration accompanied by neurodegeneration and male infertility in *pcd* mice (Kim et al., 2011; Mullen et al., 1976; Mullen and LaVail, 1975). The demonstration that the functions of connecting cilia in photoreceptors are, similar to motile cilia and flagella, dependent on tubulin glycylation, further underlines the universal importance of this specific PTM for different types of cilia in the mammalian organism.

MATERIALS AND METHODS

Animal experimentation

All wild-type control mice used in our experiments were C57BL/6 mice (Janvier-Europe). For experiments in mice lacking the TTLL3 gene, we used either the *Ttll3* mutant mice [European Mouse Mutant Archive (EMMA); mouse strain B6;B6-Ttll3<tm1a(EUCOMM)Wtsi>/Wtsi)] (Rocha et al., 2014), or *Ttll3*$^{-/-}$ mice. The latter were generated in two steps. First, we excised the *lacZ*-neomycin cassette *in vivo* by crossing B6;B6-Ttll3<tm1a (EUCOMM)Wtsi>/Wtsi) mice with a Flp-deleter line (C57BL/6N genetic background FLP under *ACTB* promoter), generating the *Ttll3*$^{flox/flox}$ strain. Next, we excised the exon 6 of *Ttll3*$^{flox/flox}$ mice by crossing them to mice expressing Cre recombinase under the control of a PGK promoter (Lallemand et al., 1998), thus generating the *Ttll3*$^{-/-}$ strain.

The Purkinje cell degeneration (*pcd*) mouse strain (BALB/cByJ-Agtpbp1*pcd*-3J-J), bearing a spontaneous mutation (Agtpbp1^{pcd}) in the *AGTPBP1* (*CCP1*) gene (Mullen et al., 1976), was obtained from the Jackson Laboratory.

Animals were maintained with access to food and water *ad libitum* in a colony room kept at constant temperature (19–22°C) and humidity (40–50%) on a 12-h-light–12-h-dark cycle. Genotyping was performed by routine PCR technique according to the EM05077 (https://www.infrafrontier.eu/sites/infrafrontier.eu/files/upload/public/pdf/genotype_protocols/EM05077_geno.pdf) EMMA protocol for TTLL3 mutant mice, and as previously described for the *pcd* strain (Rogowski et al., 2010).

All experimental procedures were performed in strict accordance with the guidelines of the European Community (86/609/EEC) and the French National Committee (87/848) for care and use of laboratory animals.

Histology

Eyes from C57BL/6 and *Ttll3*$^{-/-}$ mice were fixed by incubation in 4% paraformaldehyde in 0.1 M phosphate buffer, pH 7.4 at 4°C. The eyes were then embedded in paraffin and cut into 5-µm sections. For immunostaining, the paraffin sections were deparaffinized in Xylene and boiled in a microwave oven for two periods of 10 min in a citrate buffer (10 mM citric acid, pH 6.0). Sections were incubated with primary antibodies in antibody diluent (Dako) in a humidified chamber overnight at 4°C. Primary antibodies used were GT335 (mouse anti-glutamylated tubulin; 1:1000; AdipoGen AG-20B-0020-C100), TAP952 (mouse anti-monoglycylated tubulin; 1:100; from Anne Aubusson-Fleury, CBM, Gif-sur-Yvette, France), polyE (rabbit anti-polyglutamylation; 1:1000; Adipogen AG-25B-0030-C050), C105 (rabbit anti-β-tubulin; 1:1000; from Jose Manuel Andreu, Centro de Investigaciones Biológicas, Madrid, Spain), 20H5 (mouse anti-centrin; 1:100; Millipore AB04-1624), DM1A (mouse anti-α-tubulin; 1:1000; Sigma T6199), mouse anti-Rhodopsin (1:2000; Abcam ab3267), and rabbit anti-GFAP (1:500; Dako Z0334).

Sections were washed and incubated with a 1:200 dilution of secondary Alexa Fluor 488-conjugated anti-mouse IgG2A (Invitrogen A21131), Alexa Fluor 555 anti-rabbit (Invitrogen A31572), Alexa Fluor 633-conjugated anti-mouse IgG1 (Invitrogen A21240), or Alexa Fluor 647-conjugated anti-rabbit (Invitrogen A21244) antibodies in antibody diluent (Dako) in a humidified chamber for 2 h at room temperature in the dark.

Apoptosis was probed in fixed retinas using the In Situ Cell Death Detection Kit, TMR red (TUNEL assay; Roche, Mannheim, Germany) according to the manufacturer's instructions.

Sections were washed and counterstained with 1 µg/ml DAPI (Thermo Scientific 62248) to visualize nuclei. The sections were mounted in Fluorescent Mounting Medium (Dako) and stored at 4°C.

Microscopy

Confocal images were acquired using a Zeiss LSM 710 confocal microscope with Zen software (Zeiss, Thornwood, NY). We used 40× (NA 1.3) and 63× (NA 1.4) oil objectives. Individual channels were collected sequentially. Laser lines for excitation were 405, 488, 555 and 633 nm, and emissions were collected between 440–480, 505–550, 580–625 and 650–700 nm for blue, green, red and far-red fluorescence, respectively. All experiments were performed in triplicate, and all images were taken using the same laser power, zoom factor, image averaging and resolution. *Z*-stacks were taken with 0.35-µm steps and converted into single planes by maximum projection with ImageJ software (National Institutes of Health).

Images were mounted using ImageJ software (National Institutes of Health), and false colours were used to merge images of multiple antibody labelling. Only linear adjustments of colour intensity were performed.

Quantification of staining intensity for different tubulin-PTM antibodies and determination of the length of connecting cilia

Whole-mount preparations of adult mouse retinas stained with different antibodies specific to tubulin PTMs were used to quantify the abundance of these PTMs at different developmental stages. Retinas stained with an anti-centrin antibody (20H5) were used to measure the length of connecting cilia (this antibody specifically labels the length of connecting cilia in photoreceptors; Giessl et al., 2004; Trojan et al., 2008).

Confocal images were taken with Zeiss LSM 710. 16-bit images of 512×512 size were used for the determination of connecting-cilia length with the ObjectJ plugin (Norbert Vischer and Stelian Nastase, University of Amsterdam, Amsterdam, The Netherlands) in the ImageJ software (Bosch Grau et al., 2013).

Square regions of interest (ROIs), including inner and outer segments of photoreceptors were defined and the mean pixel intensity of staining in the masked region was corrected by subtracting background pixel intensity. A threshold of pixel intensity was set based on the comparison of staining intensity of control. The same thresholds were applied to each image analysed.

For each quantification, at least three sections from two to four retinas were analysed, and at least 30 measurements were performed per data point. Triplicate measurements were performed at each developmental stage. Data in Figs 3 and 5D represent mean±s.e.m. values between three different animals. Multiple comparisons were performed by Student's *t*-test. $P<0.05$ was considered statistically significant.

Electrophoresis and immunoblotting

Retinas were dissected from mice and homogenized in 160 µl of P300 lysis buffer (20 mM Na_2HPO_4 pH 7.0, 250 mM NaCl, 30 mM $Na_4P_2O_7$, 0.1% NP40, 5 mM EDTA and 5 mM DTT) per mouse. 40 µg of each protein sample was loaded on 7% SDS-PAGE special gels to resolve α- and β-tubulin bands (Magiera and Janke, 2013). Proteins were transferred onto nitrocellulose membranes with the Trans-Blot® Turbo™ Transfer System (BioRad). Membranes were washed in TBS containing 0.1% Tween 20 (TBS-T), and subsequently incubated with 5% fat-free milk (60 min), primary antibody (GT335, 1:6000; polyE, 1:8000; TAP952, 1:1000) in 2.5% fat-free milk in TBS-T for 1 h (or overnight at 4°C for TAP952), and secondary horseradish peroxidase (HRP)-labelled anti-mouse- or anti-rabbit-IgG antibodies (1:10,000, GE Healthcare) for 45 min. After washing with TBS-T, immuno-labelling was revealed with enhanced chemiluminescence (GE Healthcare).

In situ hybridization

Sense and antisense riboprobes were synthesized using a PCR-based *in situ* hybridization technique as previously described (Suzuki et al., 2005; Young et al., 1993). Briefly, PCR was performed with TTLL3 gene-specific primers encompassing a T7 RNA polymerase-binding site. Purified PCR products were used as templates for transcription reactions with a T7 primer and T7 RNA polymerase to generate digoxigenin-conjugated sense and antisense TTLL3 cRNAs.

Retina sections were deparaffinized by incubation in xylene, and rehydrated through a graded series of alcohol solutions. Next, 150 ng of sense or antisense cRNA probes were diluted in 150 µl of mRNA hybridization medium (HIS hybridization solution, Dako, Trappes, France) and incubated overnight at 55°C in a humidified chamber. After three washes of 30 min at 60°C with 1× Stringent Wash Concentrate (Dako), sections were incubated with 1:500 alkaline phosphatase-coupled anti-DIG antibody in antibody diluent (Dako) for 1 h at room temperature. The hybridization was then visualized with BCIP/NBT color development substrate (5-bromo-4-chloro-3-indolyl-phosphate/nitro blue tetrazolium). Stained tissue sections were mounted with Aquatex (PolyLabo, Strasbourg, France).

RNA isolation and qRT-PCR

Total RNA was isolated from retinas at different postnatal delays (P0, P4, 5 weeks, 5 months and 12 months) with the RNeasy MICRO kit (QIAGEN). Quality and concentration of total RNA was determined with a Nanodrop Spectrophotometer (Thermo Fisher Scientific).

For qRT-PCR, cDNA was synthesized with the SYBRGreen Master Mix kit. PCR amplification was performed on an ABI Prism 7900 Sequence Detection System (Perkin-Elmer Applied Biosystems, Foster City, CA) as described in detail elsewhere (Bieche et al., 1999).

qRT-PCR was performed for all known murine TTLL and CCP genes, as well as for the *TBP* gene (NM_013684) as an endogenous control. Primers are listed in Table S1, and PCR conditions are available on request. The relative mRNA expression levels of each gene, expressed as the *N*-fold difference in target gene expression relative to the *TBP* gene, and termed 'N_{target}', was calculated as $N_{target}=2^{\Delta Ct(sample)}$. The value of the cycle threshold (ΔCt) of a given sample was determined by subtracting the average Ct value of the target gene from the average Ct value of the *TBP* gene.

Histochemistry of retina sections

5-µm-thick paraffin-embedded sections of retinas were stained with haematoxylin and eosin (H&E) according to the manufacturer's protocol. The slides were dehydrated and placed on a coverslip. Brightfield images were captured with an ApoTome-equipped Axio Imager M2 microscope and processed using AxioVision REL 7.8 software (Zeiss, Oberkochen, Germany).

Acknowledgements

We thank C. Alberti, E. Belloir, F. Bertrand, T. Giordano, I. Grandjean, H. Hermange, M.M. Magiera, C. Serieyssol, A. Thadal (Institut Curie), A. Aubusson-Fleury (CBM, Gif-sur-Yvette, France), for technical assistance. We are grateful to A. Aubusson-Fleury and M. Andreu, (Centro de Investigaciones Biológicas, Madrid, Spain) for generously providing us with essential reagents, and to the EUCOMM consortium for generating and providing the *Ttll3*$^{-/-}$ mouse. We are grateful to S. Bodakuntla (Institut Curie) for instructive discussions.

Competing interests

The authors declare no competing or financial interests.

Author contributions

Conceptualization: M.B.G, C.M., C.J.; Methodology: M.B.G., C.M., S.G., S.V.; Validation: M.B.G, C.M., S.G., S.V.; Formal analysis: M.B.G, C.M., S.G., S.V.; Investigation: M.B.G, C.M., S.G., S.V.; Resources: C.R., O.T., P.M.S., C.J.; Writing – original draft preparation: M.B.G, C.M., C.J.; Writing – review and editing M.B.G, C.M., S.G., C.J.; Visualization: M.B.G, C.M., S.G., C.J.; Supervision: I.B., C.J.; Project administration: C.J.; Funding acquisition: C.M., C.R., C.J.

Funding

This work has received support under the program 'Investissements d'Avenir' launched by the French Government and implemented by the Agence Nationale de la Recherche (ANR) (references ANR-10-LBX-0038, ANR-10-IDEX-0001-02 PSL). The work of C.J. was supported by the Institut Curie (supported by the European Commission), the Fondation pour la Recherche Médicale (FRM) (research grant DEQ20081213977), the French National Research Agency (ANR) award ANR-12-BSV2-0007, the Institut National du Cancer (INCA) (grant 2009-1-PL BIO-12-IC-1 and 2013-1-PL BIO-02-ICR-1), and the Fondation Pierre Gilles de Gennes (FPGG)

for a 3T grant. C.M. was supported by Retina France, and C.R. by an FRM fellowship (FDT20120925331).

Supplementary information

Supplementary information available online at
http://jcs.biologists.org/lookup/doi/10.1242/jcs.199091.supplemental

References

Akella, J. S., Wloga, D., Kim, J., Starostina, N. G., Lyons-Abbott, S., Morrissette, N. S., Dougan, S. T., Kipreos, E. T. and Gaertig, J. (2010). MEC-17 is an alpha-tubulin acetyltransferase. *Nature* **467**, 218-222.

Alfinito, P. D. and Townes-Anderson, E. (2002). Activation of mislocalized opsin kills rod cells: a novel mechanism for rod cell death in retinal disease. *Proc. Natl. Acad. Sci. USA* **99**, 5655-5660.

Anand, M. and Khanna, H. (2012). Ciliary transition zone (TZ) proteins RPGR and CEP290: role in photoreceptor cilia and degenerative diseases. *Expert Opin. Ther. Targets* **16**, 541-551.

Arce, C. A., Rodriguez, J. A., Barra, H. S. and Caputto, R. (1975). Incorporation of L-tyrosine, L-phenylalanine and L-3,4-dihydroxyphenylalanine as single units into rat brain tubulin. *Eur. J. Biochem.* **59**, 145-149.

Arevalo, M. A., Nieto, J. M., Andreu, D. and Andreu, J. M. (1990). Tubulin assembly probed with antibodies to synthetic peptides. *J. Mol. Biol.* **214**, 105-120.

Audebert, S., Desbruyeres, E., Gruszczynski, C., Koulakoff, A., Gros, F., Denoulet, P. and Eddé, B. (1993). Reversible polyglutamylation of alpha- and beta-tubulin and microtubule dynamics in mouse brain neurons. *Mol. Biol. Cell* **4**, 615-626.

Audebert, S., Koulakoff, A., Berwald-Netter, Y., Gros, F., Denoulet, P. and Eddé, B. (1994). Developmental regulation of polyglutamylated alpha- and beta-tubulin in mouse brain neurons. *J. Cell Sci.* **107**, 2313-2322.

Bedoni, N., Haer-Wigman, L., Vaclavik, V., Tran, H. V., Farinelli, P., Balzano, S., Royer-Bertrand, B., El-Asrag, M. E., Bonny, O., Ikonomidis, C. et al. (2016). Mutations in the polyglutamylase gene TTLL5, expressed in photoreceptor cells and spermatozoa, are associated with cone-rod degeneration and reduced male fertility. *Hum. Mol. Genet.*[Epub]

Bieche, I., Onody, P., Laurendeau, I., Olivi, M., Vidaud, D., Lidereau, R. and Vidaud, M. (1999). Real-time reverse transcription-PCR assay for future management of ERBB2-based clinical applications. *Clin. Chem.* **45**, 1148-1156.

Blanks, J. C. and Spee, C. (1992). Retinal degeneration in the pcd/pcd mutant mouse: accumulation of spherules in the interphotoreceptor space. *Exp. Eye Res.* **54**, 637-644.

Blanks, J. C., Mullen, R. J. and LaVail, M. M. (1982). Retinal degeneration in the pcd cerebellar mutant mouse. II. Electron microscopic analysis. *J. Comp. Neurol.* **212**, 231-246.

Bobinnec, Y., Moudjou, M., Fouquet, J. P., Desbruyères, E., Eddé, B. and Bornens, M. (1998). Glutamylation of centriole and cytoplasmic tubulin in proliferating non-neuronal cells. *Cell Motil. Cytoskeleton* **39**, 223-232.

Bosch Grau, M., Gonzalez Curto, G., Rocha, C., Magiera, M. M., Marques Sousa, P., Giordano, T., Spassky, N. and Janke, C. (2013). Tubulin glycylases and glutamylases have distinct functions in stabilization and motility of ependymal cilia. *J. Cell Biol.* **202**, 441-451.

Boubakri, M., Chaya, T., Hirata, H., Kajimura, N., Kuwahara, R., Ueno, A., Malicki, J., Furukawa, T. and Omori, Y. (2016). Loss of ift122, a retrograde Intraflagellar Transport (IFT) complex component, leads to slow, progressive photoreceptor degeneration due to inefficient Opsin transport. *J. Biol. Chem.* **291**, 24465-24474.

Bré, M. H., Redeker, V., Quibell, M., Darmanaden-Delorme, J., Bressac, C., Cosson, J., Huitorel, P., Schmitter, J. M., Rossier, J., Johnson, T. et al. (1996). Axonemal tubulin polyglycylation probed with two monoclonal antibodies: widespread evolutionary distribution, appearance during spermatozoan maturation and possible function in motility. *J. Cell Sci.* **109**, 727-738.

Broekhuis, J. R., Leong, W. Y. and Jansen, G. (2013). Regulation of cilium length and intraflagellar transport. *Int. Rev. Cell Mol. Biol.* **303**, 101-138.

Bujakowska, K. M., Zhang, Q., Siemiatkowska, A. M., Liu, Q., Place, E., Falk, M. J., Consugar, M., Lancelot, M.-E., Antonio, A., Lonjou, C. et al. (2015). Mutations in IFT172 cause isolated retinal degeneration and Bardet-Biedl syndrome. *Hum. Mol. Genet.* **24**, 230-242.

Cambray-Deakin, M. A. and Burgoyne, R. D. (1987). Posttranslational modifications of alpha-tubulin: acetylated and detyrosinated forms in axons of rat cerebellum. *J. Cell Biol.* **104**, 1569-1574.

Chang, B., Hawes, N. L., Hurd, R. E., Davisson, M. T., Nusinowitz, S. and Heckenlively, J. R. (2002). Retinal degeneration mutants in the mouse. *Vision Res.* **42**, 517-525.

Eddé, B., Rossier, J., Le Caer, J. P., Desbruyeres, E., Gros, F. and Denoulet, P. (1990). Posttranslational glutamylation of alpha-tubulin. *Science* **247**, 83-85.

Ersfeld, K., Wehland, J., Plessmann, U., Dodemont, H., Gerke, V. and Weber, K. (1993). Characterization of the tubulin-tyrosine ligase. *J. Cell Biol.* **120**, 725-732.

Fernandez-Gonzalez, A., La Spada, A. R., Treadaway, J., Higdon, J. C., Harris, B. S., Sidman, R. L., Morgan, J. I. and Zuo, J. (2002). Purkinje cell degeneration (pcd) phenotypes caused by mutations in the axotomy-induced gene, Nna1. *Science* **295**, 1904-1906.

Giessl, A., Pulvermuller, A., Trojan, P., Park, J. H., Choe, H.-W., Ernst, O. P., Hofmann, K. P. and Wolfrum, U. (2004). Differential expression and interaction with the visual G-protein transducin of centrin isoforms in mammalian photoreceptor cells. *J. Biol. Chem.* **279**, 51472-51481.

Hallak, M. E., Rodriguez, J. A., Barra, H. S. and Caputto, R. (1977). Release of tyrosine from tyrosinated tubulin. Some common factors that affect this process and the assembly of tubulin. *FEBS Lett.* **73**, 147-150.

Handel, M. A. and Dawson, M. (1981). Effects on spermiogenesis in the mouse of a male sterile neurological mutation, purkinje cell degeneration. *Gamete Res.* **4**, 185-192.

Hao, L. and Scholey, J. M. (2009). Intraflagellar transport at a glance. *J. Cell Sci.* **122**, 889-892.

Hollingsworth, T. J. and Gross, A. K. (2012). Defective trafficking of rhodopsin and its role in retinal degenerations. *Int. Rev. Cell Mol. Biol.* **293**, 1-44.

Honjo, M., Tanihara, H., Kido, N., Inatani, M., Okazaki, K. and Honda, Y. (2000). Expression of ciliary neurotrophic factor activated by retinal Muller cells in eyes with NMDA- and kainic acid-induced neuronal death. *Invest. Ophthalmol. Vis. Sci.* **41**, 552-560.

Iandiev, I., Biedermann, B., Bringmann, A., Reichel, M. B., Reichenbach, A. and Pannicke, T. (2006). Atypical gliosis in Müller cells of the slowly degenerating rds mutant mouse retina. *Exp. Eye Res.* **82**, 449-457.

Ikegami, K. and Setou, M. (2009). TTLL10 can perform tubulin glycylation when co-expressed with TTLL8. *FEBS Lett.* **583**, 1957-1963.

Ikegami, K., Mukai, M., Tsuchida, J.-I., Heier, R. L., MacGregor, G. R. and Setou, M. (2006). TTLL7 is a mammalian beta-tubulin polyglutamylase required for growth of MAP2-positive neurites. *J. Biol. Chem.* **281**, 30707-30716.

Ikegami, K., Sato, S., Nakamura, K., Ostrowski, L. E. and Setou, M. (2010). Tubulin polyglutamylation is essential for airway ciliary function through the regulation of beating asymmetry. *Proc. Natl. Acad. Sci. USA* **107**, 10490-10495.

Janke, C. (2014). The tubulin code: molecular components, readout mechanisms, and functions. *J. Cell Biol.* **206**, 461-472.

Janke, C., Rogowski, K., Wloga, D., Regnard, C., Kajava, A. V., Strub, J.-M., Temurak, N., van Dijk, J., Boucher, D., van Dorsselaer, A. et al. (2005). Tubulin polyglutamylase enzymes are members of the TTL domain protein family. *Science* **308**, 1758-1762.

Jiang, S.-T., Chiou, Y.-Y., Wang, E., Chien, Y.-L., Ho, H.-H., Tsai, F.-J., Lin, C.-Y., Tsai, S.-P. and Li, H. (2009). Essential role of nephrocystin in photoreceptor intraflagellar transport in mouse. *Hum. Mol. Genet.* **18**, 1566-1577.

Karlstetter, M., Sorusch, N., Caramoy, A., Dannhausen, K., Aslanidis, A., Fauser, S., Boesl, M. R., Nagel-Wolfrum, K., Tamm, E. R., Jagle, H. et al. (2014). Disruption of the retinitis pigmentosa 28 gene Fam161a in mice affects photoreceptor ciliary structure and leads to progressive retinal degeneration. *Hum. Mol. Genet.* **23**, 5197-5210.

Kastner, S., Thiemann, I.-J., Dekomien, G., Petrasch-Parwez, E., Schreiber, S., Akkad, D. A., Gerding, W. M., Hoffjan, S., Günes, S., Günes, S. et al. (2015). Exome sequencing reveals AGBL5 as novel candidate gene and additional variants for retinitis pigmentosa in five Turkish families. *Invest. Ophthalmol. Vis. Sci.* **56**, 8045-8053.

Kim, N., Xiao, R., Choi, H., Jo, H., Kim, J.-H., Uhm, S.-J. and Park, C. (2011). Abnormal sperm development in pcd(3J)-/- mice: the importance of Agtpbp1 in spermatogenesis. *Mol. Cells* **31**, 39-48.

Kimura, Y., Kurabe, N., Ikegami, K., Tsutsumi, K., Konishi, Y., Kaplan, O. I., Kunitomo, H., Iino, Y., Blacque, O. E. and Setou, M. (2010). Identification of tubulin deglutamylase among Caenorhabditis elegans and mammalian cytosolic carboxypeptidases (CCPs). *J. Biol. Chem.* **285**, 22936-22941.

Konno, A., Setou, M. and Ikegami, K. (2012). Ciliary and flagellar structure and function-their regulations by posttranslational modifications of axonemal tubulin. *Int. Rev. Cell Mol. Biol.* **294**, 133-170.

Kubo, T., Yanagisawa, H.-A., Yagi, T., Hirono, M. and Kamiya, R. (2010). Tubulin polyglutamylation regulates axonemal motility by modulating activities of inner-arm dyneins. *Curr. Biol.* **20**, 441-445.

Kubo, T., Hirono, M., Aikawa, T., Kamiya, R. and Witman, G. B. (2015). Reduced tubulin polyglutamylation suppresses flagellar shortness in Chlamydomonas. *Mol. Biol. Cell* **26**, 2810-2822.

Lallemand, Y., Luria, V., Haffner-Krausz, R. and Lonai, P. (1998). Maternally expressedPGK-Cre transgene as a tool for early and uniform activation of the Cre site-specific recombinase. *Transgenic Res.* **7**, 105-112.

LaVail, M. M. (1973). Kinetics of rod outer segment renewal in the developing mouse retina. *J. Cell Biol.* **58**, 650-661.

LaVail, M. M., Blanks, J. C. and Mullen, R. J. (1982). Retinal degeneration in the pcd cerebellar mutant mouse. I. Light microscopic and autoradiographic analysis. *J. Comp. Neurol.* **212**, 217-230.

L'Hernault, S. W. and Rosenbaum, J. L. (1985). Chlamydomonas alpha-tubulin is posttranslationally modified by acetylation on the epsilon-amino group of a lysine. *Biochemistry* **24**, 473-478.

Magiera, M. M. and Janke, C. (2013). Investigating tubulin posttranslational modifications with specific antibodies. In *Methods Cell Biol*, Vol. 115 (ed. J. J. Correia and L. Wilson), pp. 247-267. Burlington: Academic Press.

Mary, J., Redeker, V., Le Caer, J.-P., Rossier, J. and Schmitter, J.-M. (1996). Posttranslational modifications in the C-terminal tail of axonemal tubulin from sea urchin sperm. *J. Biol. Chem.* **271**, 9928-9933.
Mary, J., Redeker, V., Le Caer, J.-P., Rossier, J. and Schmitter, J.-M. (1997). Posttranslational modifications of axonemal tubulin. *J. Protein Chem.* **16**, 403-407.
Morrow, E. M., Belliveau, M. J. and Cepko, C. L. (1998). Two phases of rod photoreceptor differentiation during rat retinal development. *J. Neurosci.* **18**, 3738-3748.
Mullen, R. J. and LaVail, M. (1975). Two new types of retinal degeneration in cerebellar mutant mice. *Nature* **258**, 528-530.
Mullen, R. J., Eicher, E. M. and Sidman, R. L. (1976). Purkinje cell degeneration, a new neurological mutation in the mouse. *Proc. Natl. Acad. Sci. USA* **73**, 208-212.
O'Hagan, R., Piasecki, B. P., Silva, M., Phirke, P., Nguyen, K. C. Q., Hall, D. H., Swoboda, P. and Barr, M. M. (2011). The tubulin deglutamylase CCPP-1 regulates the function and stability of sensory cilia in C. elegans. *Curr. Biol.* **21**, 1685-1694.
Ou, G., Blacque, O. E., Snow, J. J., Leroux, M. R. and Scholey, J. M. (2005). Functional coordination of intraflagellar transport motors. *Nature* **436**, 583-587.
Pathak, N., Obara, T., Mangos, S., Liu, Y. and Drummond, I. A. (2007). The zebrafish fleer gene encodes an essential regulator of cilia tubulin polyglutamylation. *Mol. Biol. Cell* **18**, 4353-4364.
Pathak, N., Austin, C. A. and Drummond, I. A. (2011). Tubulin tyrosine ligase-like genes ttll3 and ttll6 maintain Zebrafish cilia structure and motility. *J. Biol. Chem.* **286**, 11685-11695.
Piperno, G., LeDizet, M. and Chang, X. J. (1987). Microtubules containing acetylated alpha-tubulin in mammalian cells in culture. *J. Cell Biol.* **104**, 289-302.
Redeker, V., Levilliers, N., Schmitter, J. M., Le Caer, J. P., Rossier, J., Adoutte, A. and Bré, M. H. (1994). Polyglycylation of tubulin: a posttranslational modification in axonemal microtubules. *Science* **266**, 1688-1691.
Reiter, J. F., Blacque, O. E. and Leroux, M. R. (2012). The base of the cilium: roles for transition fibres and the transition zone in ciliary formation, maintenance and compartmentalization. *EMBO Rep.* **13**, 608-618.
Rocha, C., Papon, L., Cacheux, W., Marques Sousa, P., Lascano, V., Tort, O., Giordano, T., Vacher, S., Lemmers, B., Mariani, P. et al. (2014). Tubulin glycylases are required for primary cilia, control of cell proliferation and tumor development in colon. *EMBO J.* **33**, 2247-2260.
Rogowski, K., Juge, F., van Dijk, J., Wloga, D., Strub, J.-M., Levilliers, N., Thomas, D., Bré, M.-H., Van Dorsselaer, A., Gaertig, J. et al. (2009). Evolutionary divergence of enzymatic mechanisms for posttranslational polyglycylation. *Cell* **137**, 1076-1087.
Rogowski, K., van Dijk, J., Magiera, M. M., Bosc, C., Deloulme, J.-C., Bosson, A., Peris, L., Gold, N. D., Lacroix, B., Bosch Grau, M. et al. (2010). A family of protein-deglutamylating enzymes associated with neurodegeneration. *Cell* **143**, 564-578.
Sanders, M. A. and Salisbury, J. L. (1994). Centrin plays an essential role in microtubule severing during flagellar excision in Chlamydomonas reinhardtii. *J. Cell Biol.* **124**, 795-805.
Schulze, E., Asai, D. J., Bulinski, J. C. and Kirschner, M. (1987). Posttranslational modification and microtubule stability. *J. Cell Biol.* **105**, 2167-2177.
Shang, Y., Li, B. and Gorovsky, M. A. (2002). Tetrahymena thermophila contains a conventional gamma-tubulin that is differentially required for the maintenance of different microtubule-organizing centers. *J. Cell Biol.* **158**, 1195-1206.
Shida, T., Cueva, J. G., Xu, Z., Goodman, M. B. and Nachury, M. V. (2010). The major alpha-tubulin K40 acetyltransferase alphaTAT1 promotes rapid ciliogenesis and efficient mechanosensation. *Proc. Natl. Acad. Sci. USA* **107**, 21517-21522.
Sun, X., Park, J. H., Gumerson, J., Wu, Z., Swaroop, A., Qian, H., Roll-Mecak, A. and Li, T. (2016). Loss of RPGR glutamylation underlies the pathogenic mechanism of retinal dystrophy caused by TTLL5 mutations. *Proc. Natl. Acad. Sci. USA* **113**, E2925-E2934.
Suryavanshi, S., Eddé, B., Fox, L. A., Guerrero, S., Hard, R., Hennessey, T., Kabi, A., Malison, D., Pennock, D., Sale, W. S. et al. (2010). Tubulin glutamylation regulates ciliary motility by altering inner dynein arm activity. *Curr. Biol.* **20**, 435-440.
Suzuki, T., Akimoto, M., Mandai, M., Takahashi, M. and Yoshimura, N. (2005). A new PCR-based approach for the preparation of RNA probe. *J. Biochem. Biophys. Methods* **62**, 251-258.
Tort, O., Tanco, S., Rocha, C., Bieche, I., Seixas, C., Bosc, C., Andrieux, A., Moutin, M.-J., Xavier Aviles, F., Lorenzo, J. et al. (2014). The cytosolic carboxypeptidases CCP2 and CCP3 catalyze posttranslational removal of acidic amino acids. *Mol. Biol. Cell* **25**, 3017-3027.
Trojan, P., Krauss, N., Choe, H.-W., Giessl, A., Pulvermüller, A. and Wolfrum, U. (2008). Centrins in retinal photoreceptor cells: regulators in the connecting cilium. *Prog. Retin. Eye Res.* **27**, 237-259.
van Dijk, J., Rogowski, K., Miro, J., Lacroix, B., Eddé, B. and Janke, C. (2007). A targeted multienzyme mechanism for selective microtubule polyglutamylation. *Mol. Cell* **26**, 437-448.
Veleri, S., Lazar, C. H., Chang, B., Sieving, P. A., Banin, E. and Swaroop, A. (2015). Biology and therapy of inherited retinal degenerative disease: insights from mouse models. *Dis. Model. Mech.* **8**, 109-129.
Wensel, T. G., Zhang, Z., Anastassov, I. A., Gilliam, J. C., He, F., Schmid, M. F. and Robichaux, M. A. (2016). Structural and molecular bases of rod photoreceptor morphogenesis and disease. *Prog. Retin. Eye Res.* **55**, 32-51.
Wloga, D., Rogowski, K., Sharma, N., Van Dijk, J., Janke, C., Edde, B., Bré, M.-H., Levilliers, N., Redeker, V., Duan, J. et al. (2008). Glutamylation on alpha-tubulin is not essential but affects the assembly and functions of a subset of microtubules in Tetrahymena thermophila. *Eukaryot. Cell* **7**, 1362-1372.
Wloga, D., Webster, D. M., Rogowski, K., Bré, M.-H., Levilliers, N., Jerka-Dziadosz, M., Janke, C., Dougan, S. T. and Gaertig, J. (2009). TTLL3 is a tubulin glycine ligase that regulates the assembly of cilia. *Dev. Cell* **16**, 867-876.
Wloga, D., Dave, D., Meagley, J., Rogowski, K., Jerka-Dziadosz, M. and Gaertig, J. (2010). Hyperglutamylation of tubulin can either stabilize or destabilize microtubules in the same cell. *Eukaryot. Cell* **9**, 184-193.
Wolff, A., de Nechaud, B., Chillet, D., Mazarguil, H., Desbruyeres, E., Audebert, S., Eddé, B., Gros, F. and Denoulet, P. (1992). Distribution of glutamylated alpha and beta-tubulin in mouse tissues using a specific monoclonal antibody, GT335. *Eur. J. Cell Biol.* **59**, 425-432.
Wright, A. F., Chakarova, C. F., Abd El-Aziz, M. M. and Bhattacharya, S. S. (2010). Photoreceptor degeneration: genetic and mechanistic dissection of a complex trait. *Nat. Rev. Genet.* **11**, 273-284.
Young, I. D., Stewart, R. J., Ailles, L., Mackie, A. and Gore, J. (1993). Synthesis of digoxigenin-labeled cRNA probes for nonisotopic in situ hybridization using reverse transcription polymerase chain reaction. *Biotech. Histochem.* **68**, 153-158.

Supplementary Material for:

Alterations in the balance of tubulin glycylation and glutamylation in photoreceptors leads to retinal degeneration

Montserrat Bosch Grau, Christel Masson, Sudarshan Gadadhar, Cecilia Rocha, Olivia Tort, Patricia Marques Sousa, Sophie Vacher, Ivan Bieche and Carsten Janke

medium and strong expression levels

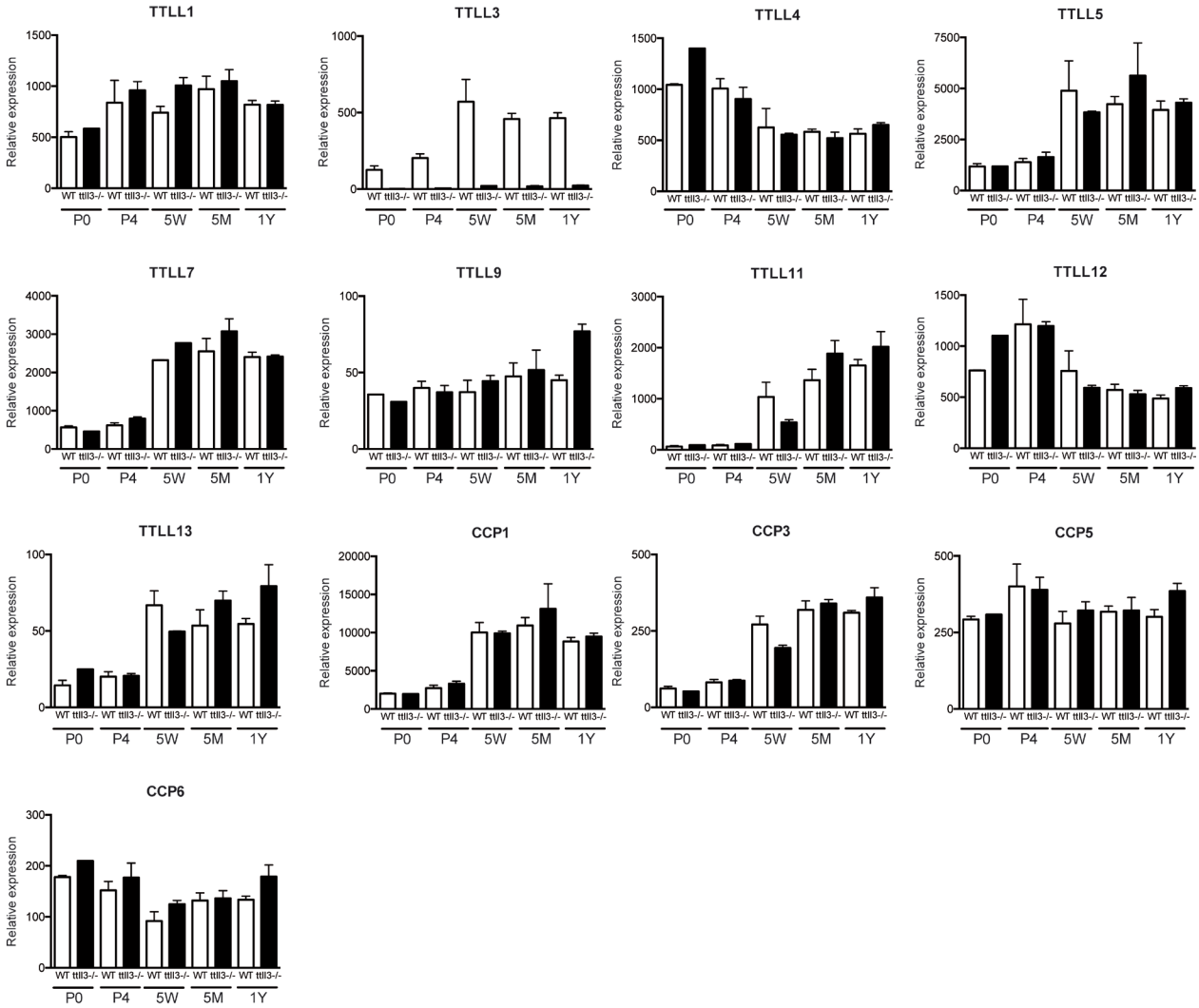

very low expression levels

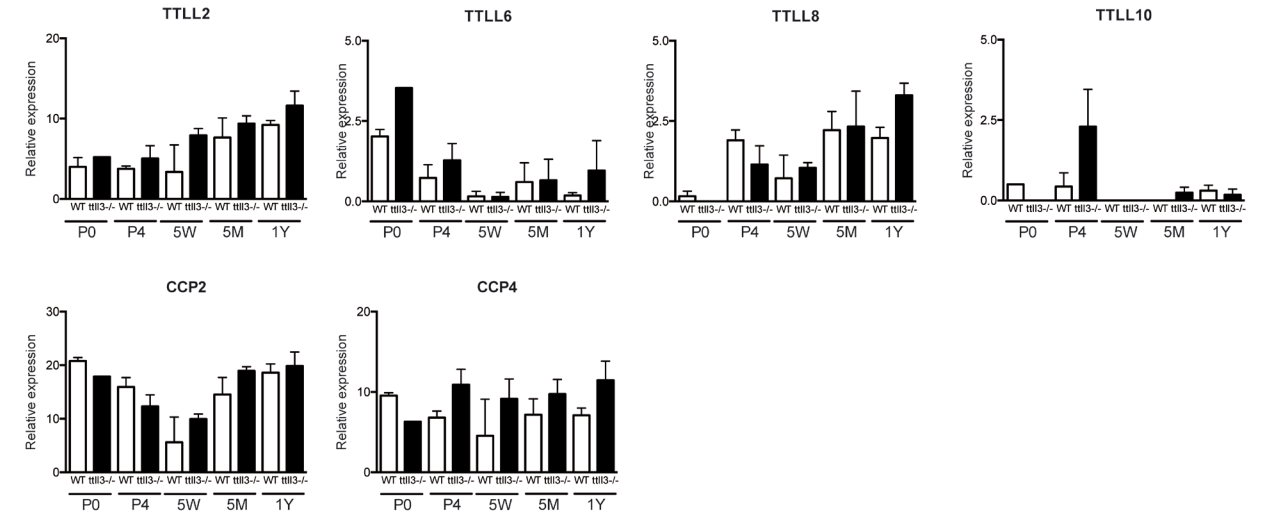

Supplementary Figure S1: TTLL3 is the only initiating glycylase expressed in mouse retina at all developmental stages.
The relative mRNA expression levels of TTLL and CCP genes were analysed by qRT-PCR in retina samples from control and *Ttll3*$^{-/-}$ mice at different postnatal ages. The samples were analysed by qRT-PCR, and values were standardized to expression levels of the TBP gene. Mean values ±SEM of two independent mRNA samples are shown. TTLL and CCP gene expression was classified as “strong/medium” or “very low” expressed. The data of the very-low-expressed genes cannot be considered reliable due to the low values. TTLL3 is not expressed in the *Ttll3*$^{-/-}$ mice retina at any developmental stage. TTLL8 is not reliably quantifiable (only detectable at very low transcript levels). None of the TTLL and CCP genes are significantly up- or down-regulated in the *Ttll3*$^{-/-}$ retina as compared to the control retina.

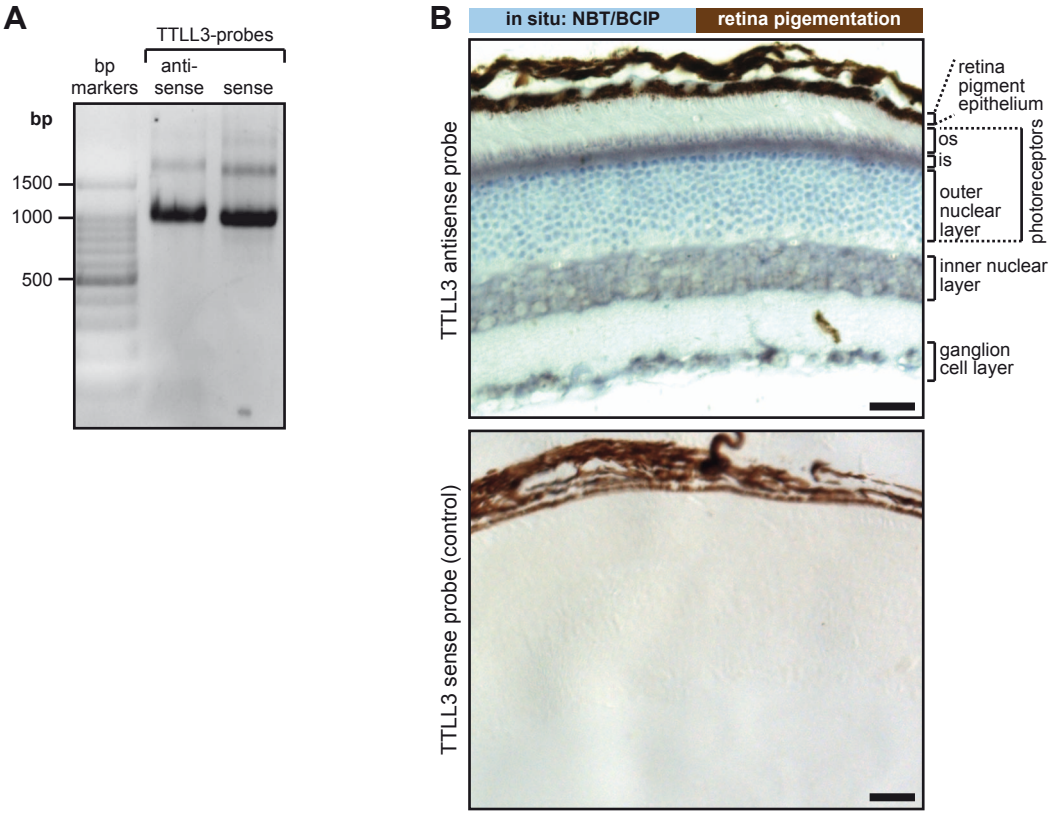

Supplementary Figure S2: TTLL3 expression in adult mouse retina

A) RNA probes for in situ hybridization were synthesized, and checked in 0.8% agarose gel electrophoresis stained with ethidium bromide. The size of the molecular weight markers is indicated. **B**) *In situ* hybridization of retinal sections from adult mouse with DIG-labelled antisense and sense (negative control) probes. The probes were detected with anti-DIG antibody. Note the particularly strong labelling of nuclei in the photoreceptors – outer nuclear layer. Scale bar 20 µm. Abbreviations: is: inner segment, os: outer segment.

TTLL3 expression is prominent in the photoreceptor layer, which was consistent with the strong TAP952 immunoreactivity in connecting cilia of the photoreceptors (Fig. 1B). Surprisingly however, TTLL3 transcripts were also found in the cells of the inner nuclear layer, and within ganglion cell layer, both structures in which no obvious glycylation signal was detected with the TAP952 antibody (Fig. 2B). This situation is reminiscent of our previous observations in colon, where TTLL3 is expressed and plays a key role in controlling primary cilia and epithelia proliferation, while no TAP952-positive MT structures were found (Rocha et al., 2014). One possible explanation is that TAP952, which was raised against *Paramecium* tubulin (Callen et al., 1994), does not detect all glycylated epitopes on mammalian tubulin, and might preferentially detect cilia-specific glycylation patterns (Bré et al., 1996).

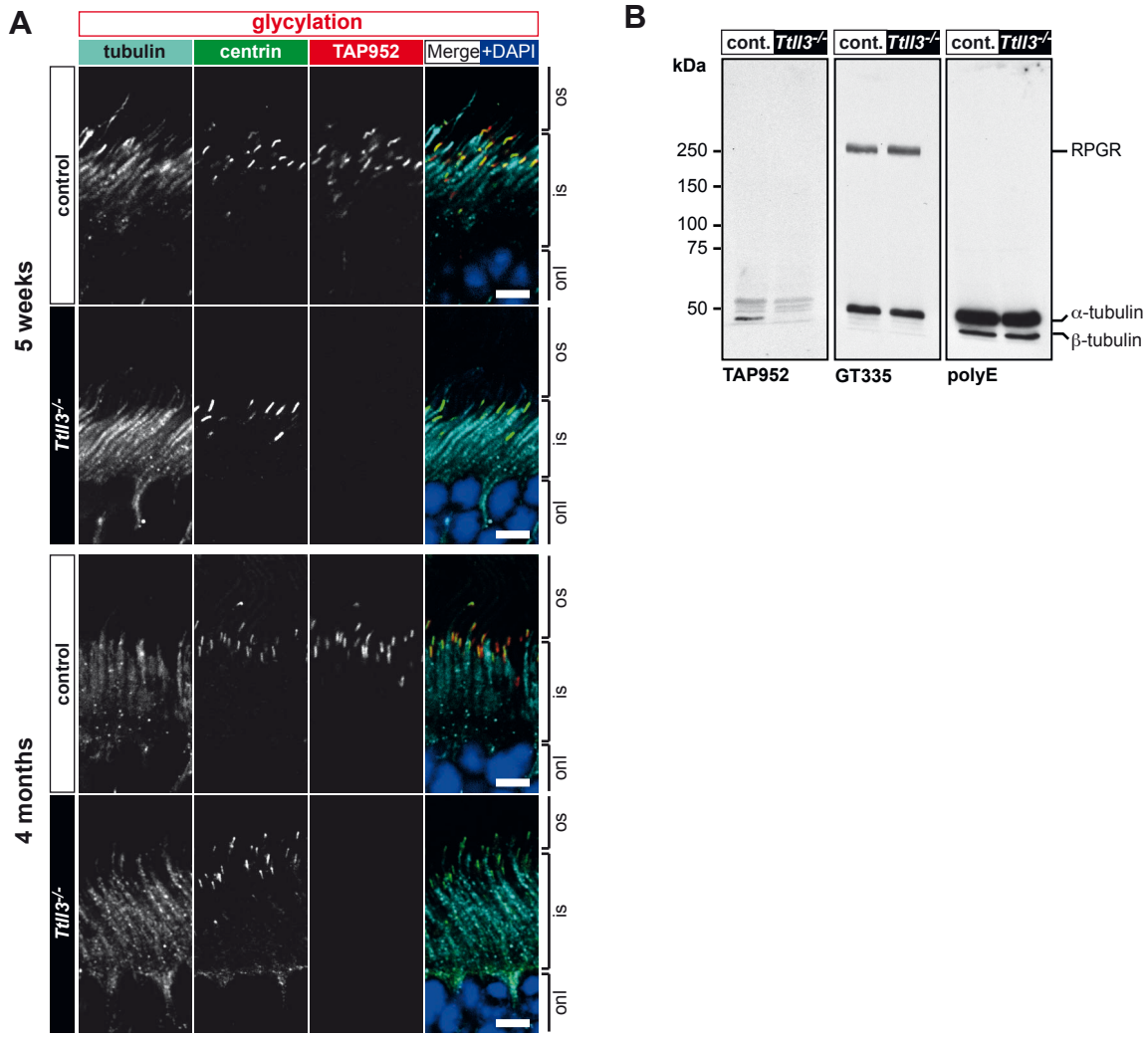

Supplementary Figure S3: Absence of glycylation in the *Ttll3*$^{-/-}$ mouse retina

A) Co-immunostaining of retina sections from control and *Ttll3*$^{-/-}$ mice at different postnatal ages with pan-centrin antibody (20H5; green), β-tubulin (C105; cyan) and anti-glycylation TAP952 (red). Nuclei were visualized with DAPI (blue). TAP952 labelling is completely absent in the *Ttll3*$^{-/-}$ mouse. Scale bars 5 µm. Abbreviations: is: inner segment, os: outer segment, onl: outer nuclear layer. **B**) Retinas dissected from control and *Ttll3*$^{-/-}$ mice were homogenized and resolved in 7% SDS-PAGE gels, followed by immunoblot. A GT335-reactive protein of 250 kDa, most likely RPGR (Sun et al., 2016) is detected at equal intensity in both, control and *Ttll3*$^{-/-}$ retinas. TAP952 detects a specific protein band (β-tubulin) only in control, but not in *Ttll3*$^{-/-}$ retina. Note that the very strong labelling of α- and β-tubulin with GT335 and polyE most likely originates to a large extent from the neurons in the retina, thus, differences in glutamylation levels that have been detected in the photoreceptors (Fig. 2, 3) are overwritten by the neuronal tubulin in the blot.

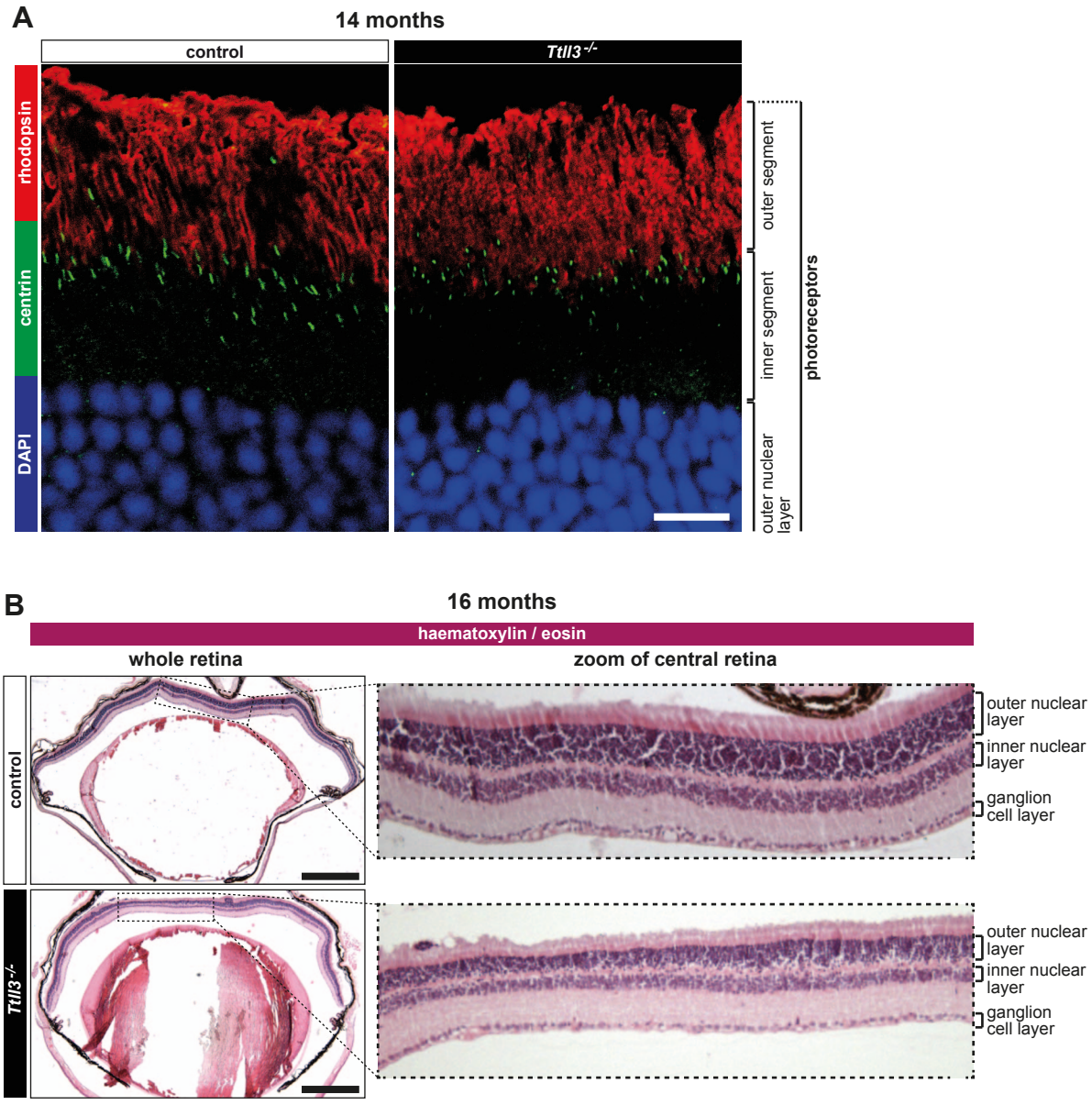

Supplementary Figure S4: Verification of connecting cilia length measurements and retina thickness comparison

A) To control for the correct orientation of our retina tissue sections during the length measurements (Fig. 2, 3), control and *Ttll3*$^{-/-}$ retina sections from 12-month-old mice were labelled with pan-centrin (20H5; green) to visualize the connecting cilia and the basal bodies, and with an anti-rhodopsin antibody (red) for the outer segments. Nuclei were labelled with DAPI (blue). Note that the connecting-cilia (20H5) length is reduced in *Ttll3*$^{-/-}$ retina while the outer-segment length is comparable to control. This demonstrates that our measurement procedure for determining the length of connecting cilia was not biased by the orientation of the histological blocks. Scale bar 10 µm.

B) Paraffin-embedded retinal sections of 16-month-old control and *Ttll3*$^{-/-}$ mice were stained with haematoxylin and eosin. In the whole-retina view, outer regions of both retinas appear of similar thickness, while the central part of the retina is thinner. The significant thinning of the outer nuclear layer in the central retina of *Ttll3*$^{-/-}$ mice becomes evident in the zoom images. Scale bar 500 µm.

Supplementary Table S1: Primer pairs used for RT-qPCR

Primer names	Forward primer (5'-3')	Reverse primer (5'-3')
TTLL1-Mm	ATTCCCGACTGCAAGTGGAACA	CTGGGCCAGCTCCTCGTCAT
TTLL2-Mm	GGTCTGCAGAGTTTGGGTGATGT	TCTTCAAAGGCTTGCTTTCCTGTA
TTLL3-Mm	GGAGGGGGATCGGAACATCT	CATCTCATCCAGGCGGTTCAT
TTLL4-Mm	CCATGGAAACAAGCTCAAAGGAGTA	CAGTGGGGCTGAGTCAGAGACAA
TTLL5-Mm	GCGCCTCTATGTGCTCGTGACT	TGCGGATGTTCTTGGAGCCTT
TTLL6-Mm	GGGACGATTCTTGCAGCAGTGT	ATGGCCTGGAAACCCTTGACTT
TTLL7-Mm	GTACATCCCACCAAACGAGTCCA	TGCTGCCTTTGTCTTCAGTTTCAT
TTLL8-Mm	GAATGGAATGACCTGACACAGCAGTA	ACTTTTCGAATCAGTGATGGAAGCA
TTLL9-Mm	CCGCTTCAAGACCACCCTCAT	GCCAGCTGACATCACACCAATAGA
TTLL10-Mm	CCCAGTACCCAAACCAAGGTCCT	AAGCCTGCCTCTCGTCTCTGATGT
TTLL11-Mm	ACCAGCGGGACTCAGGGATGT	CATGGAGAGGTTGCAGCTTGAACT
TTLL12-Mm	CATCCCTCAGTTTGAGAAGCAGTA	GCCTTGAAGATCTCAGCCTGAA
TTLL13-Mm	CCTGGGGTTTGACATCTTACTGGA	AAGCTTGGGGAGTGGTTTACCTCTA
AGBL1-Mm	GCAGCATTGCTGAAATCCAAGTCTA	GCGGCTGTGCCAGTCCTGA
AGBL2-Mm	AATCTGCAGAAAGCCGTCAGAGT	AGTGTGTTTGTCCGTGTAGAGGTCA
AGBL3-Mm	CTGTTTACCCAAACTCCAAGGAAGAT	GGATGTTCGGTTACCCCCAACT
AGBL4-Mm	CCAAGAGTCTTTACCGAGATGGGAT	CTGTGGTCTGGGCAGCGATAGT
AGBL5-Mm	GCACCCAAAAGGTCAGCCAT	GCCGCCTTCTGTCTGAGCA
AGTPBP1-Mm	TTCCACAGAGTCAGATACTGCCAGAT	CAGAACTTCCATGCCTGTAGAACCT
TBP-Mm	CCCTTGTACCCTTCACCAATGAC	TCACGGTAGATACAATATTTTGAAGCTG

References

Callen, A.-M., Adoutte, A., Andrew, J. M., Baroin-Tourancheau, A., Bré, M.-H., Ruiz, P. C., Clérot, J.-C., Delgado, P., Fleury, A., Jeanmaire-Wolf, R. et al. (1994). Isolation and characterization of libraries of monoclonal antibodies directed against various forms of tubulin in Paramecium. *Biol. Cell* **81**, 95-119.

Bré, M. H., Redeker, V., Quibell, M., Darmanaden-Delorme, J., Bressac, C., Cosson, J., Huitorel, P., Schmitter, J. M., Rossier, J., Johnson, T. et al. (1996). Axonemal tubulin polyglycylation probed with two monoclonal antibodies: widespread evolutionary distribution, appearance during spermatozoan maturation and possible function in motility. *J. Cell Sci.* **109**, 727-738.